ECONSTOR
Make Your Publications Visible.

A Service of

ZBW Leibniz-Informationszentrum Wirtschaft
Leibniz Information Centre for Economics

Ojea-Ferreiro, Javier; Panzica, Roberto Calogero; Papadopoulos, Georgios

Working Paper

Climate stress test of the global supply chain network: The case of river floods

JRC Working Papers in Economics and Finance, No. 2025/9

Provided in Cooperation with:
Joint Research Centre (JRC), European Commission

Suggested Citation: Ojea-Ferreiro, Javier; Panzica, Roberto Calogero; Papadopoulos, Georgios (2025) : Climate stress test of the global supply chain network: The case of river floods, JRC Working Papers in Economics and Finance, No. 2025/9, European Commission, Ispra

This Version is available at:
https://hdl.handle.net/10419/334949

Standard-Nutzungsbedingungen:

Die Dokumente auf EconStor dürfen zu eigenen wissenschaftlichen Zwecken und zum Privatgebrauch gespeichert und kopiert werden.

Sie dürfen die Dokumente nicht für öffentliche oder kommerzielle Zwecke vervielfältigen, öffentlich ausstellen, öffentlich zugänglich machen, vertreiben oder anderweitig nutzen.

Sofern die Verfasser die Dokumente unter Open-Content-Lizenzen (insbesondere CC-Lizenzen) zur Verfügung gestellt haben sollten, gelten abweichend von diesen Nutzungsbedingungen die in der dort genannten Lizenz gewährten Nutzungsrechte.

Terms of use:

Documents in EconStor may be saved and copied for your personal and scholarly purposes.

You are not to copy documents for public or commercial purposes, to exhibit the documents publicly, to make them publicly available on the internet, or to distribute or otherwise use the documents in public.

If the documents have been made available under an Open Content Licence (especially Creative Commons Licences), you may exercise further usage rights as specified in the indicated licence.


https://creativecommons.org/licenses/by/4.0/

WWW.ECONSTOR.EU

Mitglied der Leibniz-Gemeinschaft

European Commission

Climate stress test of the global supply chain network: the case of river floods

JRC Working Papers in Economics and Finance, 9/2025

Ojea Ferreiro, J., Panzica, R., Papadopoulos, G.

2025

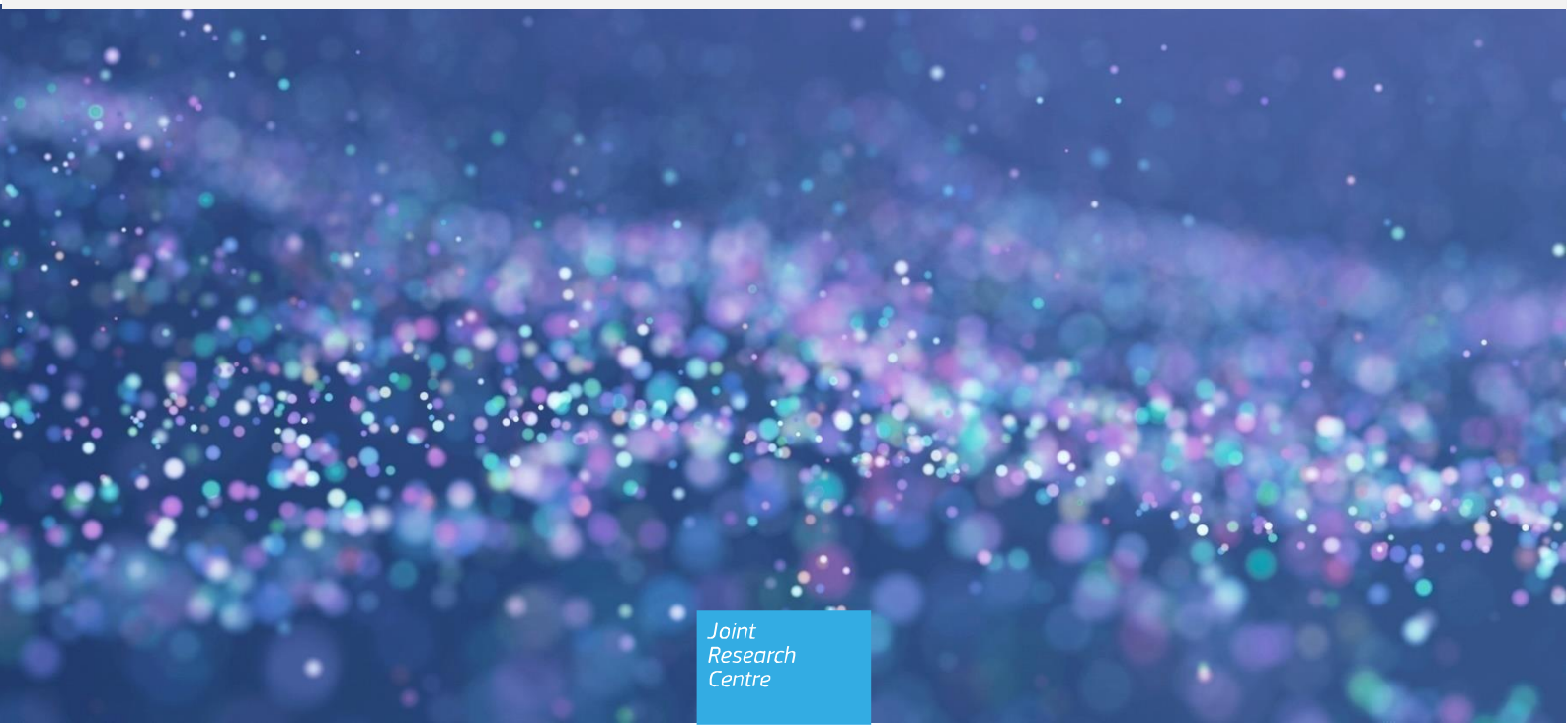

Joint Research Centre

This document is a publication by the Joint Research Centre (JRC), the European Commission's science and knowledge service. It aims to provide evidence-based scientific support to the European policymaking process. The contents of this publication do not necessarily reflect the position or opinion of the European Commission. Neither the European Commission nor any person acting on behalf of the Commission is responsible for the use that might be made of this publication. For information on the methodology and quality underlying the data used in this publication for which the source is neither Eurostat nor other Commission services, users should contact the referenced source. The designations employed and the presentation of material on the maps do not imply the expression of any opinion whatsoever on the part of the European Union concerning the legal status of any country, territory, city or area or of its authorities, or concerning the delimitation of its frontiers or boundaries.

Contact information
Name: Georgios Papadopoulos
Email: georpapadopoulos@bankofgreece.gr; gpapad.gr@gmail.com

EU Science Hub
https://joint-research-centre.ec.europa.eu

JRC141288

Ispra: European Commission, 2025

© European Union, 2025

The reuse policy of the European Commission documents is implemented by the Commission Decision 2011/833/EU of 12 December 2011 on the reuse of Commission documents (OJ L 330, 14.12.2011, p. 39). Unless otherwise noted, the reuse of this document is authorised under the Creative Commons Attribution 4.0 International (CC BY 4.0) licence (https://creativecommons.org/licenses/by/4.0/). This means that reuse is allowed provided appropriate credit is given and any changes are indicated.

For any use or reproduction of photos or other material that is not owned by the European Union permission must be sought directly from the copyright holders.

How to cite this report: Ojea Ferreiro, J., Panzica, R. and Papadopoulos, G., *Climate stress test of the global supply chain network: the case of river floods,* European Commission, Ispra, 2025, JRC141288.

Contents

Climate stress test of the global supply chain network: the case of river floods*

Javier Ojea-Ferreiro †
Roberto Panzica ‡
Georgios Papadopoulos§¶

Abstract

This study investigates how extreme flood events can indirectly impact the global supply chain through production disruptions. Using a data-driven, agent-based network model that combines company-level data with flood hazard maps, the research simulates the transmission and amplification of shocks. The findings emphasize that the size of inventories is crucial; a lean-inventory system leads to faster shock propagation, higher losses, and fewer recoveries compared to an abundant-inventory system. Additionally, the study identifies that the number and criticality of flooded companies' trade links, along with the magnitude of the flood, correlate with the speed and severity of contagion. Interestingly, a key metric -the average criticality of affected firms' outgoing links- consistently peaks before the onset of the shock's fast-propagation regime. This could serve as an early warning indicator, giving businesses and policymakers precious time to react. By identifying these critical vulnerabilities, this research provides a framework for enhancing the resilience of global supply chains in the face of increasing climate-related and other risks.
Keywords: climate risk; supply chain; floods; agent-based; data-driven
***JEL classification*:** C60; C63; D85; Q54

1 Introduction

"When France sneezes, the rest of the Europe catches a cold."[1] Although said in an era quite different from the current one, the essence of von Metternich's remark captures well a feature of modern-day economies. That, in an interconnected system, a systemic event's consequences can be felt far from its origin.

While interconnectedness can be beneficial for a system's robustness by absorbing negative shocks of relatively small magnitude, it also enables the propagation of large shocks, amplifying their impact (Acemoglu et al., 2015). This has been emphatically demonstrated in the case of financial networks during the Global Financial Crisis of 2008 and documented in the research that followed (Summer, 2013; Huang et al., 2013; Glasserman and Young, 2015; Battiston et al., 2016; Glasserman and Young, 2016; Jackson and Pernoud, 2021; Vodenska et al., 2021, and references within).

*The analytical work has been completed while the authors were working at the Joint Research Centre of the European Commission, Italy. The views expressed are those of the authors and do not necessarily reflect those of the Bank of Greece, the Bank of Canada, the Bank of Portugal, the Joint Research Centre or the European Commission. All errors and omissions are ours.

†Bank of Canada; e-mail: JOjeaFerreiro@bank-banque-canada.ca
‡Bank of Portugal; e-mail: RPanzica@bportugal.pt
§Joint Recearch Centre, European Commission
¶Bank of Greece; e-mail: GeorPapadopoulos@bankofgreece.gr (corresponding)

[1]Klemens von Metternich (ca. 1830), Austrian diplomat and statesman.

Another canonical example of a network structure in economics is the supply chain network[2]. Like in the case of financial networks, the respective literature has expanded in the wake of major disruptive events.

A well studied example is the Great East Japan earthquake[3] in 2011. Carvalho et al. (2021), quantified the significance of input-output linkages as a mechanism for the propagation and amplification of shocks. Their findings indicate that the Tōhoku earthquake led to a 0.47 percentage point decrease in Japan's real GDP growth in the year following the disaster. Boehm et al. (2019) examined how the Tōhoku earthquake of 2011 affected the US affiliates of Japanese firms affected by the earthquake. The authors documented significant output falls of roughly one-for-one with the decline of imports, in the months following the shock. Interestingly, Freund et al. (2022) find that importing firms in the automobile and electronic sectors did not re-shore or nearshore production and did not increase import diversification to mitigate risk, post-earthquake. While the replacement of suppliers from Japan did occur, it was driven mainly by fundamentals, to countries where economies of scale could be achieved.

Another event whose ripple effects have been thoroughly examined are the floods in Thailand, which also occurred in 2011. Haraguchi and Lall (2015) documented large decreases in the sales of affected companies' trade partners in the automobile and electronics sectors. In particular, Malaysia's sales of automobiles exhibited decreases of up to 25% in year-on-year terms until April 2012. In the Philippines, sales of cars declined by 4%, as a result of the lack of imports from Thailand. In the electronics industry, equally large declines were observed. Hard disk drive shipments decreased by 30% annually, which resulted to price increases by 80% to 190%. Similarly, Forslid and Sanctuary (2023) document that sales by Swedish firms with suppliers from Thailand dropped 8% in 2012, as a result of the flood. This finding highlights that propagation of shocks through the supply chain amplifies their magnitude and extends far beyond the original source.

In a study examining the indirect impact of various natural disasters, Barrot and Sauvagnat (2016) find that shocks to suppliers drop the sales of their customers by 2–3 percentage points. Importantly, this drop is stronger when the disrupted supplier is producing hard-to-substitute inputs, in which case the shock propagates further.

While the previous events affected directly mostly a single country, the recent COVID-19 pandemic exposed the serious weaknesses in global supply chains, especially in medical equipment and semiconductors for car manufacturers(Ramani et al., 2022). The impact's magnitude was such that the literature suggested that stress test exercises, similar to the ones carried out for the banking sector, should be developed to assess the resilience of companies' supply chains in the event of a crisis (Ivanov and Dolgui, 2022; Simchi-Levi and Simchi-Levi, 2020).

In that regard, several studies develop simulation models to generate insights about the mechanisms involved and investigate the impact of various scenarios. The main modelling approaches include input-output (IO) models, computational general equilibrium (CGE) models and agent-based network models[4].

Pichler et al. (2022) developed a dynamic IO model to investigate the economics and epidemiology of various scenarios for a phased restart of the UK economy. The pandemic impacted both supply and demand, with input-output constraints playing a pivotal role in constraining economic output. In this context, the level of input criticality, measured as the importance for the customer's production function over a two-month period, is crucial.

Using a CGE model, Arriola et al. (2020) find that while re-localisation of global value chains would make countries less exposed to foreign shocks, it would also hamper

[2]The term *production network* is also used by the literature. Although both terms refer to interconnected systems of firms, there do exist subtle differences between them. Since the results from both literature strands are relevant for the current study, the two terms can be used interchangeably.

[3]Also known as the Tōhoku earthquake.

[4]For some early literature and discussion about the advantages and disadvantages of each approach see Haraguchi and Lall (2013)

their capacity to absorb disruptions through trade thus making them less efficient and less stable.

In the context of natural disasters, the study by Fahr et al. (2024) is a recent example of an IO model used to quantify the indirect impact of climate-related hazards under an extremely adverse scenario. The authors find that in the event the shock materializes globally at the same time, aggregate GDP losses in the Euro Area would be more than 10% of GDP, with considerable heterogeneity across countries.

The current study is closer to the literature strand which uses agent-based network models to simulate the propagation of shocks through the supply chain[5]. Research shows that, while IO and CGE models can offer valuable insights, models at the sector level cannot appropriately capture firm-to-firm interactions and the complex ways that natural disasters affect supply chains (Hallegatte, 2019). In particular, Diem et al. (2024) demonstrated that utilizing the detailed structure of non-aggregated firm-level production networks (FPNs) provides more accurate estimations of losses compared to those derived from aggregated industry-level production networks (IPNs). In a scenario inspired by COVID-19, they modeled the shock based on detailed firm-level data during the early stages of the pandemic. Their findings indicate that employing IPNs instead of FPNs results in underestimates of losses of up to 37%.

The study by Inoue and Todo (2019) is quite revealing. The authors develop a very detailed agent-based model of the observed supply chains of about one million firms in Japan to estimate the direct and indirect effects of a historical as well as a simulated earthquake event. They find that the indirect effects of the disasters on production due to propagation are more than 20 times larger than their direct effects.

In a similarly detailed network model, Diem et al. (2022) reveal that a few companies have substantial importance for a large share of the national economic production. Importantly, firm size alone cannot explain their importance but it's rather their position in the production networks which matters most. Moreover, the study demonstrates that using aggregated sector-level data does not yield an appropriate picture of companies' systemic risk. An extension of the model by Tabachová et al. (2024) shows that economic shocks to firms propagate in the supply chain network and have ramifications for banks' equity buffers through loan defaults. Hence, contagion through the supply chain network is relevant for financial stability and realistic credit risk assessment.

Finally, research has shown that production networks can transmit shocks beyond those purely associated with production such as monetary policy (Ozdagli and Weber, 2023) or induce inflation co-movement across countries (Auer et al., 2019).

Recognizing the critical role of supply chains, policymakers at the EU level have taken a number of actions to understand dependencies and enhance EU's and Member States' strategic autonomy. In that regard, the European Commission in 2021, has identified 137 strategic products for which the European Union depends significantly on imports from third countries [6]. It has also developed specific tools to to monitor the evolution of supply chains in the EU and identify potential signal of distress (Bonnet and Ciani, 2023; Amaral et al., 2022). In addition, on March 2023, the European Commission proposed a comprehensive set of actions to ensure the EU's access to a secure, diversified, affordable and sustainable supply of critical raw materials with the goal is to crate a secure and resilient EU critical raw materials supply chains[7]. Similarly, to ensure a swift response to supply chain disruptions, the EU implemented the European Chips Act,[8] with the aim of enhancing the resilience of the Chips

[5]In production management and operations research literature, the downstream cascade of disruptions in the supply chain has been extensively studied under the term *ripple effect* (Dolgui et al., 2018). While elaborate models have thoroughly examined several aspects of it, data-driven approaches and the quantification of the ripple effect are topics at the forefront of the research agenda which still require further investigation (Dolgui and Ivanov, 2021).

[6]Commission Staff Working Paper Strategic dependencies and capacities (SWD(2021) 352 final)

[7]`https://eur-lex.europa.eu/resource.html?uri=cellar:903d35cc-c4a2-11ed-a05c-01aa75ed71a1.0001.02/DOC_1&format=PDF`

[8]Regulation (EU) 2023/1781 of the European Parliament and of the Council.

Ecosystem.

The model developed in this study is a data-driven, agent-based network model, based on actual customer-supplier relations, at a global level. Combined with forward-looking, granular, geospatial information on river floods aims to investigate the transmission, amplification and indirect impact of severe, yet plausible, flood-related shocks on firms' production. While data challenges inevitably exist, the results can offer valuable assistance to policymakers to identify where vulnerabilities lie in the supply chain, which factors influence their impact and, possibly, give them some time to implement measures to enhance the resilience of the entire supply-chain network or its specific branches.

2 Data

The study uses several data as input to the simulation model. These can be divided into two broad categories: (i) company-level data, such as their trade relationships and balance sheet information; and (ii) flood-scenario data, such as flood hazard maps and river basin information.

2.1 Company-level data

2.1.1 Supply chain information

The study uses supply chain data from FactSet Supply Chain Relationship database[9]. This database contains binary, directed, links between firms. Each link represents a trade relationship between two firms, with its direction indicating the customer-supplier role of the parties involved. However, the trading amount or more specific information about the type of products or services traded, are not reported. The study identified and extracted the full supply chains in which at least one counterparty is headquartered in the European Union, United States, or Canada, focusing on those that were active as of February 2022. The final number of companies is about 74500 with more than 230000 directed links between them. Figures 1 and 2 show the numbers, shares and direction of trade relationships, grouped by continent[10] and NACE sector, respectively.

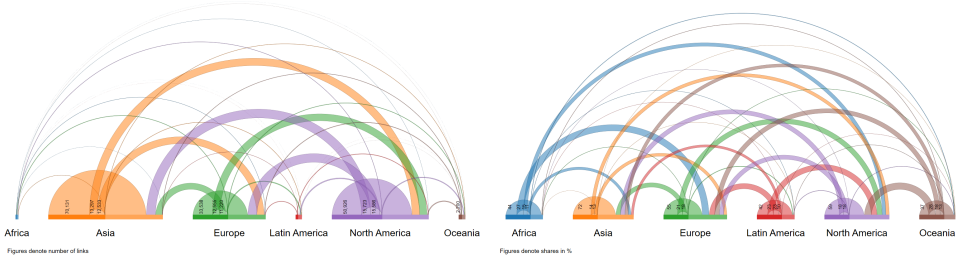

Figure 1: Numbers (left panel), shares (right panel) and direction of trade relationships, grouped by continent.

Figure 1 reveals several patterns. First, the bulk of trade relationships is between companies headquartered in Asia, North America and Europe. Second, most links occur intra-continentally, with the respective shares being half of a continent's total links, on average, ranging from 37% in Oceania to more than 70% in Asia. Finally, outgoing links from Asia to Europe and North America are similar in absolute numbers

[9] https://www.factset.com/marketplace/catalog/product/factset-supply-chain-relationships

[10] Data from Central and South America have been combined into a single group, "Latin America," due to the small number of links (and companies) from these regions.

with the respective incoming ones, yet in terms of shares they are fewer by about 5 percentage points.

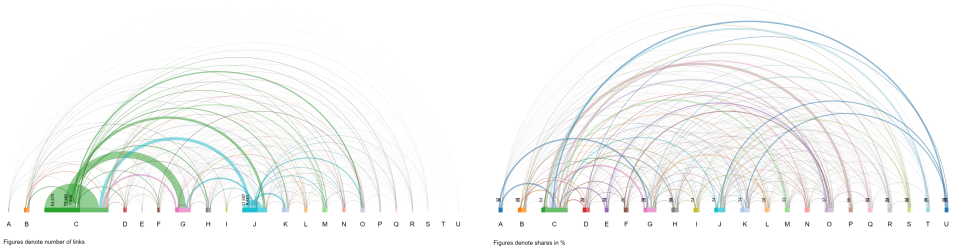

Figure 2: Numbers (left panel), shares (right panel) and direction of trade relationships, grouped by NACE sector.

Figure 2 presents a similar pattern. Manufacturing firms (C) dominate in numbers of trade links, followed by those in information & communication (J) and those in wholesale & retail trade and repair of motor vehicles (G). Similarly to continent-grouped data, trade is usually the largest within sectors, although the respective figures are generally lower, averaging at 17%.

2.1.2 Input criticality

One fundamental piece of information is how significant a company's input is for its customers' production. Recognizing that not every input is equally important for a firm's production, the study uses information from Pichler et al. (2022) where the authors conducted a survey to assess how essential an input of a given industry is for another industry's production[11].

The survey asked analysts to rate whether production in industry X can continue in case input Y is not available for two months. The outcome is an asymmetric table with rows denoting the inputs provided from industry Y to industry X, in the respective column. Each cell contains a rating of how essential industry Y's input is for industry X's production. This rating, called criticality, assumes three values; 1 for critical; 0.5 for important, but not critical; and 0 for non-critical inputs.

Based on the information from Pichler et al. (2022), the current study assigns a criticality score to each link between two companies, according to their NACE 2-digit sectors. The production function described in section 3.3.1 utilizes this criticality score to determine output decrease in case of input shortages.

Figure 3 illustrates the average criticality of links between companies from one continent to those in another.

[11]The industries in Pichler et al. (2022) correspond to ISIC 2-digit sectors, which are largely equivalent to and directly comparable with NACE 2-digit classifications.

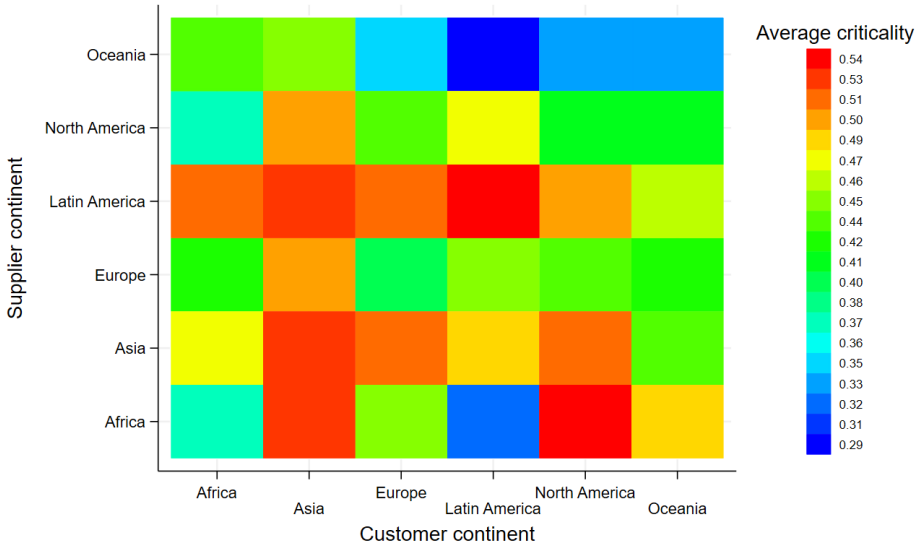

Figure 3: Average criticality of trade relationships, by continent. The horizontal axis denotes continents and the vertical one the continent of input origin. Warmer colors indicate higher criticality.

The graph in Figure 3 reveals some interesting features. First, the continent supplying the least critical inputs to its counterparties is Oceania. On the contrary, links from Asia and Latin America are the most important ones, on average. Europe and North America are in the middle. They provide more essential inputs to Asia but less so in the remaining continents. Interestingly, although most trade relationships form intra-continentally, those seem to be the least critical ones for firms' production -with the exception of Asia and Latin America- as the colors in Figure 3's secondary diagonal indicate.

2.1.3 Other company information

Finally, information on companies' geographical locations and their available inventories is essential. The former have been identified by matching FactSet with ORBIS databases through company International Securities Identification Number (ISIN) or Legal Entity Identifier (LEI) information.[12] Subsequently, the study retrieved from ORBIS matched firms' latitude and longitude coordinates either directly or through their address information.[13]

Information on company inventories has been collected from FactSet and is reported in days of inventory on hand (DOH). DOH indicates the number of days a company needs to utilize the average inventory available at its disposal. Evidently, inventories are crucial because their size influences how long can a company continue its production undisturbed in the event of input shortages.

However, information on DOH is available only for about 3% of the company sample. Thus, the analysis imputes the missing data based on the sectoral distribution of

[12]Where ISIN and LEI information is missing and only the firm name is available in any of the two databases, the study applies a fuzzy matching algorithm to identify which firm has the same name, is located at the same country and belongs to same sector. Whenever more than one institution with the same name is found, as it could be for the case of subsidiaries, the biggest one is selected.

[13]It should be noted that this information refers to companies' headquarters. Since there doesn't exist a database with the precise locations of company factories, the study uses the available information on their headquarters to geolocate them. Anecdotal evidence suggests that financial intermediaries and regulators follow the same approach when assessing company exposure to physical risk.

available datapoints. In particular, it considers two polar cases; lean[14] and abundant inventories. In both cases the study samples missing data in every simulation run from a uniform distribution. In the lean-inventory case, the distribution ranges between the DOH's sector-specific minimum and its respective first quartile, i.e. $DOH_{i,s}^{lean} = U(DOH_s^{min}, DOH_s^{Q1})$, where s is company i's NACE 2-digit sector. In the case of abundant inventories, the distribution spans between the DOH's sector-specific third quartile and its associated maximum, i.e. $DOH_{i,s}^{abundant} = U(DOH_s^{Q3}, DOH_s^{max})$.

2.2 Flood scenario

The purpose of each flood scenario is to identify which locations are prone to river floods, determine the magnitude of these events, single out the companies that would be directly affected and, finally, assess the direct impact on the latter. To achieve this, the study combines information from different datasets.

2.2.1 Flood hazard data

The basic source for the flood scenario are the river flood hazard maps at global scale developed by the Joint Research Centre (Dottori et al., 2016). It is a collection of datasets which depicts areas around the world that could be affected by river flood events of various magnitudes. They have been developed using hydrological and hydrodynamic models, driven by climatological data. Among the available occurrence frequencies, the study uses maps of events with 1-in-100-year return period. This corresponds to floods of such magnitude that their -current[15]- probability of occurring or being exceeded in any given year is 1%. This strikes a balance between high-frequency (e.g. 1-in-10 year) and very rare (e.g. 1-in-500 year) events. Figure 4 shows the global flood hazard map for events with 1-in-100-year return period.

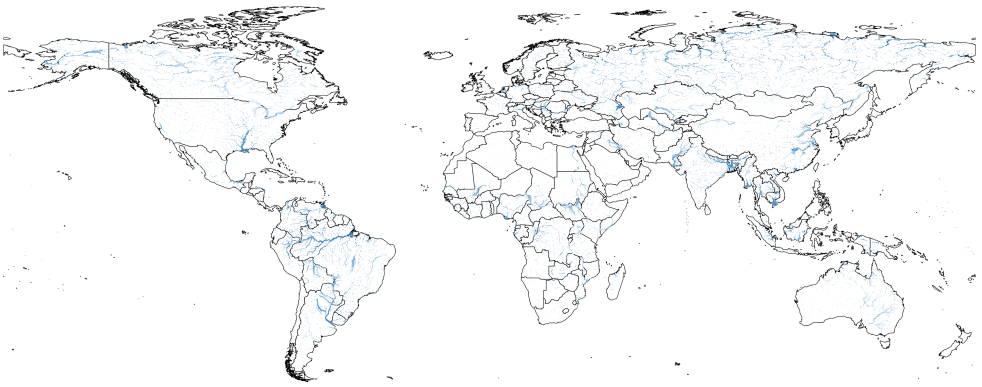

Figure 4: Global flood hazard map of 1-in-100-year return period. Darker shades denote higher water level. Country boundaries layer by the World Bank Official Boundaries dataset.

Each cell in the map in Figure 4 has a resolution of about 1 km^2 and the shades denote water depth ranging from 0.01 to 30 meters. The study uses the return period of 1-100-years, as it provides the best compromise between event frequency and associated impact. Appendix A provides a more detailed description of the dataset.

[14] Associated with the just-in-time inventory management method which focuses on keeping as low levels of inventory as possible.

[15] Return periods are estimated using historical records. Evidently, changes in the underlying conditions such as climate and land use will alter the frequency and magnitude of flood events thus resulting in the revision of these figures.

An overlay of flood hazard maps of different magnitude with companies' locational data provides an assessment of each flood event's direct impact. This information guides the choice of the specific return period for the implementation of the flood scenarios.

Table 1 shows the number of affected companies and two quantities that should influence their shock propagation capacity. The first one is the mean out-degree, which measures how many outgoing trade links the directly affected firms have, on average. Mean criticality shows the average importance of these links.

Table 1: Number of directly affected companies and metrics of their shock propagation capacity.

Return period	**N**	**Mean out-degree**	**Mean criticality**
1-in-10 year	1912	9.36	0.52
1-in-20 year	2024	9.51	0.52
1-in-50 year	2130	9.50	0.52
1-in-100 year	2214	9.53	0.52
1-in-200 year	2375	9.17	0.52
1-in-500 year	2437	9.12	0.52

Note: Based on flood hazard map data by the Joint Research Centre, FactSet data and authors' calculations.

Table 1 shows that while the sample of flooded companies shows an average increase of 5% in size by flood magnitude, the overall capacity to transmit the flood shock does not substantially change. The mean number companies' out-links peaks in the 1-in-100 year flood magnitude and then drops, whereas their importance to their customers -proxied by their average criticality- remains constant.

The observations from Table 1[16] suggest that the initial impact should be fairly stable across flood magnitudes and that the 1-in-100 year one is an informative choice exhibiting a balance between event frequency and associated impact.

2.2.2 River basin data

To develop a consistent scenario it is essential to identify which companies would be simultaneously affected by a flood event. Thus, the high-resolution, flood hazard map data need to be spatially grouped. The intuition is that any single flood event should happen around a specific river's basin. Therefore, river basins are used for appropriately grouping flood hazard data. Their boundaries come from the HydroBASINS database (Lehner and Grill, 2013). It contains information on the boundaries and areas of river sub-basins at various, hierarchically nested, breakdowns globally. From the available sub-basin breakdown levels, this study uses the middle one to group the flood map data into individual scenarios. This choice yields the closest match between the resulting average sub-basin area and the estimated average flood extent of about 900 historical, large flood events (Tellman et al., 2021). Figure 5 provides an overview of the resulting global sub-basins at the selected breakdown level.

[16] And Tables 6 and 7, in Appendix A.

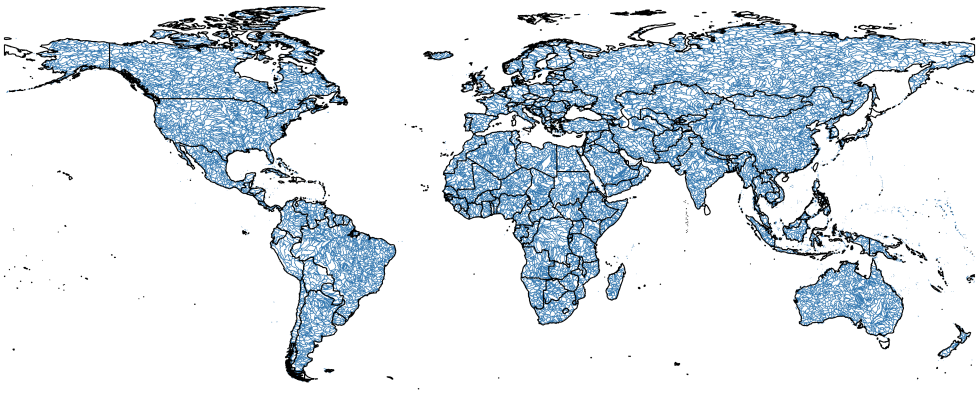

Figure 5: Global river sub-basin boundaries (blue lines). Country boundaries layer by the World Bank Official Boundaries dataset.

From the almost 16.1k individual sub-basins shown in Figure 5, this study uses only those which encompass potentially flooded companies to develop each scenario. Appendix B further describes river basin information used and discusses the rationale behind the choices made.

2.3 Linking flood scenario with company information

The intersection between firms' geographical coordinates and the flood hazard data of the chosen magnitude determines which ones will be affected. Grouping the latter by river basin results in 244 distinct scenarios. Table 2 provides some figures which describe their severity, such as water depth reached, their country extent, the number of directly affected companies and their customers. Appendix **??** gives detailed information on each scenario.

Table 2: Individual scenario statistics.

	Min	**Mean**	**Median**	**Max**
# of companies	1.00	6.93	2.00	160.00
Total out-degree	1.00	66.16	10.50	1848.00
Mean criticality	0.00	0.52	0.50	1.00
# of intersecting countries	1.00	1.19	1.00	4.00
Water depth (m)	0.01	3.95	2.25	30.00

Note: Based on HydroBASINS data, flood hazard map data by the Joint Research Centre, company-level data from FactSet and authors' calculations.

Table 2 shows that the average scenario includes about 7 flooded firms which have around 10 customers each, resulting in a mean figure of 66 customers. However, there is substantial heterogeneity as the ranges suggest. The respective maximum figures indicate that there are scenarios which can include up to 160 flooded companies which are directly connected to more than 1800 customers. It should be noted that from a total of 2214 directly affected companies, 523 are the terminal nodes in their respective supply chains. Therefore, they cannot propagate the flood shock downwards. These companies have not been considered in the initial shock. The average flood scenario's magnitude is about 4 meters and is, generally, a single-country event. Nevertheless, there are some events which extend to up to four countries. Appendix B elaborates on the relevant data and further discusses scenario design.

Two associated quantities need to be estimated in order to operationalize each scenario; the magnitude of direct damage to affected companies; and their respective restoration time.

2.3.1 Depth-damage function

To estimate the direct impact of floods to companies the study uses depth-damage functions[17] which link flood damage with specific water depths per class of structure.

It employs the damage functions developed by Huizinga et al. (2017) which provide globally consistent, continent-specific information on the fractional damage of water depth for six broad structure classes[18]. The most relevant classes among those available are commercial buildings, industrial buildings and agriculture[19].

Companies have been allocated into these three classes according to their NACE sectoral classification. The industrial building class includes firms in NACE sectors B to F; the commercial building class those in NACE sectors G to U; and, finally, agriculture those in NACE sector A. It should be noted that about 6% of the sample lacks sectoral classification information. Out of that, only about 12% has data on their location coordinates hence, only those firms can be considered in the initial flood shock. These companies have been allocated in the industrial damage class.

Based on the previous allocation scheme, the sample is almost equally split between the commercial and industrial damage classes. More specifically, about 50% belongs to the commercial and 49% to the industrial damage class while agriculture makes up less than 1% of the total. Appendix C provides a brief description of the corresponding sectoral classification in Table 9 and presents in detail the various damage functions, by continent and structure class.

2.3.2 Flood recovery

Each directly affected company requires some time to return to its previous functionality. However, relevant information in the literature is very scarce. This study uses input from the Federal Emergency Management Agency's (FEMA) Hazus flood model (FEMA, 2022). It provides information on the maximum restoration time (in days) as a function of water depth for various building types.

Time-to-recover (TTR)[20] estimates are based on expert opinion and they reflect the duration of a number of associated processes such as physical restoration of the damage, clean-up and delays because of contractor availability among others (FEMA, 2022). They are step-functions of flood depth and are grouped into ten categories, each one including several structure types. To use them, similarly to the damage functions, companies are allocated into the relevant structure type according to their sectoral classification.

Almost two thirds of the sample belong to three, broad, TTR groups. The most populated one, making up 31% of the total, includes mostly commercial-type building categories such as professional and financial services, some medical services and the public sector. The other two include heavy industry and agriculture companies (16%) and those classified in the food, drugs and chemicals industries (16%). About 2% of the potentially flooded company sample (i.e. those companies that are directly affected under the flood scenario) does not have any sectoral classification information. These cases have been assigned into the group with the most balanced recovery time pattern. Appendix D gives more information on the sectoral mapping to different structures and the maximum recovery times per building group.

[17] Known also as depth-damage curves or, simply, damage functions. This study uses these terms interchangeably.

[18] Also referred to as *damage classes*.

[19] The remaining three damage classes are residential buildings, transport facilities and infrastructure.

[20] Also known as *recovery time* or *restoration time*. This study uses these terms interchangeably.

3 Model

To examine the propagation of shocks through the global supply chain, the study uses an agent-based, network model. Companies are the network's nodes while its edges are the directed links between firms, representing their supplier-customer relationships.

3.1 Overview

The model is similar to the class of epidemiological models known as susceptible-exposed-infected-susceptible (SEIS). All companies are susceptible to experience production reductions as a result of input shortages from their suppliers. Input shortages occur primarily due to flood events while secondary ones propagate through the supply chain network. When a company reduces its output, its customers become exposed and utilize their inventories to keep providing their customers with the original level of output for as long as their inventories permit. Once exposed companies exhaust their inventories they reduce their production (i.e. become "infected"). Thus, they expose their customers to an input shock which, in turn, forces them to make use of their inventories to retain their production, eventually initiating a new cycle of the disruption's transmission. Different from the typical SEIS models and in line with the literature, the impact of the shocks on companies' production is a continuum (Inoue and Todo, 2019; Diem et al., 2022, 2024, among others). Also, a company might experience multiple shocks simultaneously due to the existence of cycles and indirect connection paths in the supply chain network. Finally, the reverse process takes generally place when the initially affected firms recover from the original shock.

Each time step corresponds to one day and each simulation runs for a short- to medium-term period which allows for each scenario's effects to unfold. The study assumes a static network, i.e. companies do not change their trade partners because of the materialized or anticipated input shortages. The literature provides some evidence in favor of that, at least in the short term (Martin et al., 2023; Freund et al., 2022; Arriola et al., 2020; Boehm et al., 2019). Thus, by focusing the analysis on the short-run dynamics strengthens the plausibility of the static-network assumption (Tabachová et al., 2024).

3.2 Initial state and flood shock

For simplicity, the study assumes that in the original state companies are at their full operational capacity which they cannot increase, at least in the short term. In every subsequent step, companies' output is a fraction of this original production level depending on the available share of inputs. Each simulation initializes the network according to the companies' actual attributes, such as their location, their trade links and balance sheet data. Since only information on the upper bounds of TTR is available, firms' TTR_i is sampled in every simulation run from a uniform distribution $U(0, TTR_c^{max})$, where c the TTR class that company i belongs to, described in Table 10.

Subsequently, the simulation sets N_0 specific companies as flooded according to the scenarios described in Table **??**. Based on the water depth's level and firms' damage class, flooded companies proportionally reduce their production, according to the respective damage-function. Their production remains at these lower levels for a period determined by TTR_i. This exposes flooded companies' customers to an input shock which affects their output if $TTR_i > DOH_j$, where DOH_j is customer j's remaining days of available inventory.

3.3 Shock propagation and impact

The study considers only downstream effects, i.e. those transmitted from suppliers to their customers and not vice versa. However, while upstream effects play a role, the

literature suggests that are the downstream ones which dominate in the presence of non-linearities in the production function (Diem et al., 2022).

The original shock propagates through the nodes of those branches in the supply chain that satisfy the following condition:

$$TTR_i > \sum_{j \in B} DOH_j$$

, where i the flooded companies and j their customers which belong to each specific branch, B, of the supply chain. Input shortages force exposed companies to utilize their inventories to maintain their original production level thus gradually reducing their remaining DOH_j. When they exhaust their inventories, they decrease their production to a fraction of their full capacity and transmit the input shock to the branch's next downstream members. In the simulation, the process iterates either for a period which allows the contagion to properly develop[21] or until the flooded firms' recovery restores the supply chain network to its original state. Obviously, if $TTR_i < DOH_k$, where k the flooded companies' immediate customers, the shock never propagates.

The appropriate damage function determines the flooded companies' output reduction, while a production function controls the magnitude of each secondary input shortage's impact on the affected companies.

3.3.1 Production function

The study assumes that the inputs supplied at $t = 0$ determine a company's maximum production level. At $t+1$, firm i's production will be a share of the original, depending on the relative amount of inputs received by its suppliers and their criticality.

In particular, a composite Leontief production function, similar to the ones described in Diem et al. (2022, 2024); Pichler et al. (2022)[22], determines companies' relative production level. It is a mix of a linear and a Leontief production function, depending on the supplier's criticality to its customer's production recognizing that not every input is equally important. The following equation defines it:

$$x_i(t+1) = min \left[\min_{k \in S^{crit}} \left(\prod_{i,k}(t) \right), \frac{1}{N} \sum_{k \in S^{all}} \prod_{i,k}(t) \right]$$

The first term describes the minimum, relative, input received by firm i from its critical suppliers, $k \in S^{crit}$. The second term is the overall, relative, amount of inputs which firm i receives from both its critical and non-critical suppliers $k \in S^{all}$. In the absence of more detailed information regarding supplied products or their volumes, the linear part of the production function applies the standard approach in the respective literature (Schueller et al., 2022; Chakraborty et al., 2024; Diem et al., 2024), imposing reductions to be proportional to the relative reduction of inputs, divided by the number of suppliers a company has. Chakraborty et al. (2024) checked the robustness of the production function's latter part and the resulting shock propagation mechanism against detailed value added tax data. They found that it provides an adequate approximation of the more accurate network representation which considers link weights based on traded volumes between partners. Figure 19 in Appendix E shows a schematic example of the production disruption's downstream cascade.

[21] In the vast majority of cases this period is one year. However, in few occasions the simulation horizon needs to be extended by a couple of years to get a clearer picture of the shock's propagation.

[22] And supported by empirical evidence. Higher input specificity results in more sticky firm-to-firm relationships (Martin et al., 2023). Moreover, the results in Barrot and Sauvagnat (2016) suggest that while the Cobb-Douglas production function may be an adequate approximation at the industry level, it may be less so at the micro level, where substitutable inputs coexist with difficult-to-substitute inputs.

4 Results

The simulation performs 50 runs on each scenario and takes the average outcome for the following metrics: the total number of affected companies (N); their average maximum out-criticality (C^{out}_{max});[23]; and the total relative output lost (L). To examine the sectoral distribution of shocks' propagation, the study also breaks the relative output lost down by companies' NACE 2-digit sector. Affected companies are those whose production at any time t is less than 100%.

4.1 Some general patterns

Figure 6 shows some representative examples of the model's output for the two inventory size cases examined, over two scenarios of different severity.

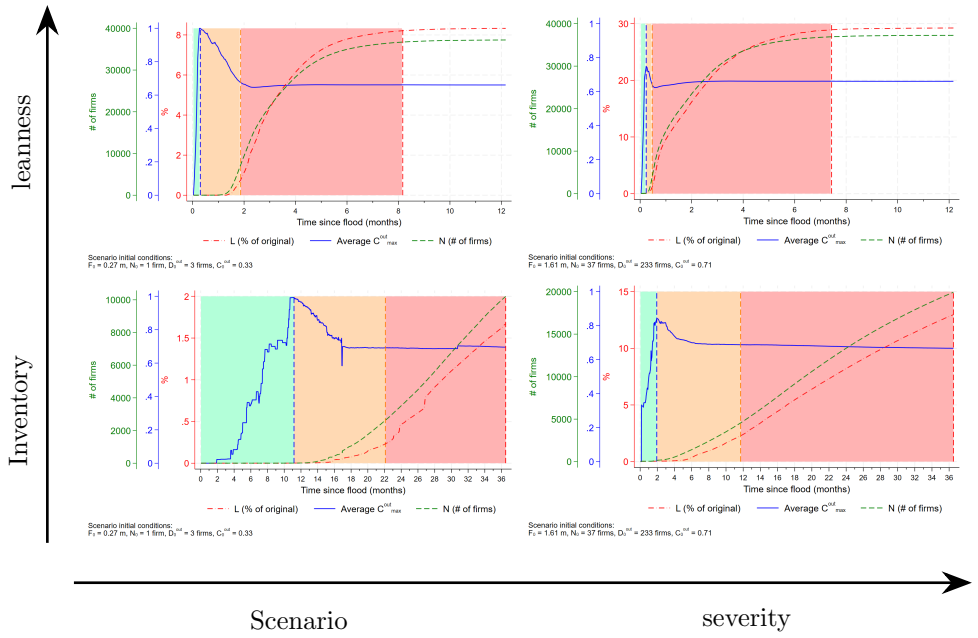

Figure 6: Representative evolution of the number of affected companies, relative output lost and average criticality. Rows denote scenario severity and columns inventory leanness. Each metric is the average over 50 simulation runs for the same scenario. The green-shaded area is the very low contagion regime, until C^{out}_{max} peaks. The orange-shaded area is the time between C^{out}_{max}'s peak and the point in time until which contagion's speed remains slow. The red-shaded area denotes the onset of the fast-pace contagion regime until the cascade's plateau.

The most notable pattern in Figure 6 is the markedly different pace in the shock's transmission between the abundant and the lean inventory cases. As expected, the latter evolves quickly, with the number of affected companies and the lost output plateauing after a few months. On the contrary, in the abundant inventory case the disruption propagates much more gradually, with the graphs suggesting that its peaks occur beyond the end of the simulation horizon, more than a year after the flood's initial trigger.

Two key moments help characterize the evolution of the disruption's transmission through the supply chain. The first one, t^*_N, is the point in time at which the shock's cascade changes from a slow moving regime to a fast paced one[24]. The second, t^{max}_N,

[23]Out-criticality is the criticality of a firm's links for its customers. Therefore, $C^{out}_{i,max}$ is the maximum criticality of company i's outgoing links.

[24]Marked in the plot as the vertical, orange line.

marks the moment when the disruption reaches its saturation point and, practically, stops spreading further[25]. During the period defined by these two moments the number of affected firms increases by several orders of magnitude, from very few to tenths of thousands. To identify t_N^* and t_N^{max} the analysis fits the following 3-parameter logistic function to the number of affected companies:

$$N_i(t) = \frac{a_i}{1 + e^{-b_i(t-c_i)}}$$

, where $N_i(t)$ the number of affected companies at time t for each scenario, i. The maximum of the previous function's second derivative defines the onset of the high-contagion regime, t_N^*. The point in time when the fitted curve becomes flat marks the second moment, t_N^{max}. While saturation strictly happens at the limit, as $\lim_{t\to+\infty} N_t(t) = a_i$, in practice the curve is sufficiently flat when $N_i(t) = 0.999a_i$. Another important quantity is the time t_C^* at which the affected companies' average criticality exhibits its maximum. As Figure 6 shows, it precedes t_N^* by a non-trivial amount thus performing as an early warning indicator. The study further examines this in Section 4.5.

4.2 The role of inventories

As Figure 6 indicates, the size of inventories plays a crucial role in mitigating the shock's impact by smoothing its transmission through the supply chain. The following paragraphs examine their role in the disruption's cascade and impact.

4.2.1 Contagion spread speed

The contagion spreads at noticeably different speeds, depending on firms' inventory size. Both distributions of high-contagion regime's onset and its duration, until the saturation point, presented in Figure 7 indicate that in the case of lean inventories the propagation of the shock occurs earlier and evolves at a considerably faster pace compared to the abundant inventories.

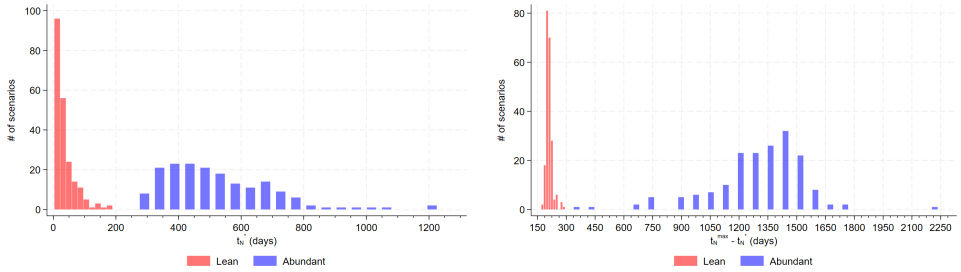

Figure 7: Distribution of scenarios' time to high-contagion (left panel) and the high-contagion regime's duration (right panel) by inventory size.

In particular, in the lean-inventory case the majority of scenarios reaches the high-contagion regime within less than 2 months, while even the most benign ones extend to about 6 months, as the left panel in Figure 7 shows. On the contrary, this occurs at a much later stage in the abundant-inventory case. The earliest start of the high-contagion regime is at about 9 months after the initial shock, while in most scenarios this takes more than a year to happen, with a few slow-moving ones exhibiting a t_N^* larger than 3 years.

Another distinctive feature of the two cases is the notable difference in the high-contagion regime's duration; the time needed to reach its saturation point, after its onset. In the lean-inventory case this period lasts, on average, 7 months and certainly less than 10 months. Instead, contagion's evolution develops at a much slower pace

[25]Marked in the plot as the vertical, red line.

in the abundant-inventory case. It takes about 3.5 years, on average, with scenarios exhibiting a range between 1 and 6 years, to reach the saturation point after entering into the high-contagion regime.

It is worth mentioning again the modelling assumption of a fixed supply chain network and absent shock-mitigating policy actions during the simulation period. Evidently, this is less plausible in the long horizons involved in the abundant-inventory case. However, the results should better reflect actual situations in a lean-inventory world given the short time frames -from few days to few months- during which actions would be less likely to be implemented or, even more, bear fruit. Moreover, they highlight the different time scales associated with the two inventory sizes and indicate how much shorter the time buffer for response from policymakers or other agents would be.

4.2.2 Impact

To gauge each scenario's impact, the study uses the supply chain network's relative output lost[26] at a specific point in time, based on the production function described in Section 3.3.1. The most appropriate moment is the start of the high-contagion regime, at $t = t_N^*$, because it occurs early in time. This has two advantages; the figures in both inventory size cases are less affected by the static network and no-policy-action assumptions; and it happens well within the simulation horizon, hence extrapolation is not needed to get an estimate but one can directly use the simulation's output, instead. Figure 8 presents the distribution of relative output loss (L^*) by inventory size for the flood scenarios examined.

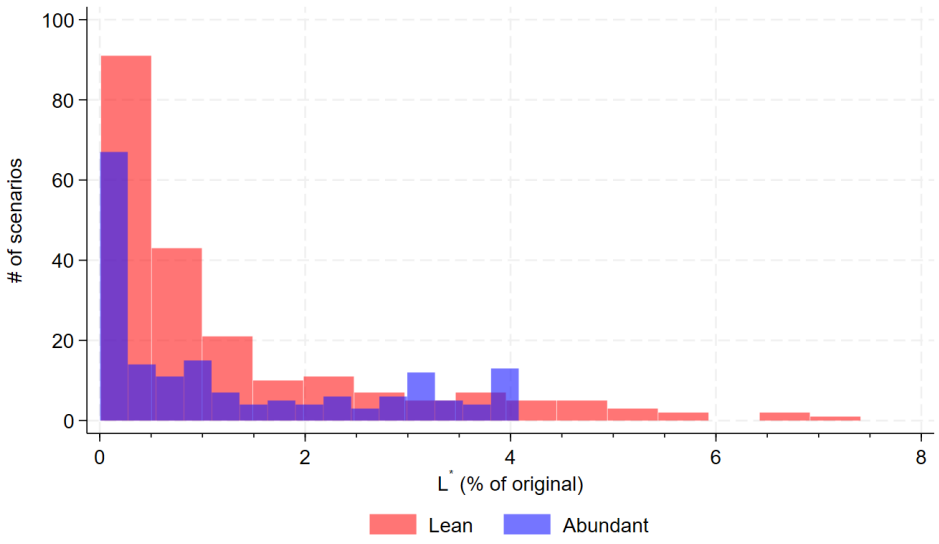

Figure 8: Distribution of scenarios' output loss (L^*) at $t = t_N^*$ as a share of the original, by inventory size.

The two distributions in Figure 8 overlap substantially. In particular, the L^*s from the abundant-inventory case are completely contained by the lean-inventory ones. However, the distribution of the latter shows a longer tail, beyond the former's maximum at 4%, reaching almost twice as far, at 7.5%. Combined with the previous analysis of the contagion's speed, this suggests that the losses in the lean-inventory case will be higher and will materialize within a couple of months as opposed to the abundant-inventory one where relevant time scales are in the order of a year or more.

[26] As a share of the original. Appendix E provides an example of shock's propagation and its impact.

In addition to the aggregate losses over the whole supply chain network, the analysis examines their sectoral distribution by breaking them down by NACE 2-digit sector in Section 4.4.

4.2.3 Recovery

During the simulation, the reverse of the shock's propagation can occur if the flooded firms recover to their original status thus providing again their customers the needed inputs. This depends on two key factors. The flooded companies' TTR, which determines the time needed for their recovery, and the size of their customers' inventories -along the affected supply chain- which slows down the shock's transmission. Figure 9 presents the number of scenarios which result in contagion as well as the non-contagious ones (recovered and recoverable[27]), by inventory size.

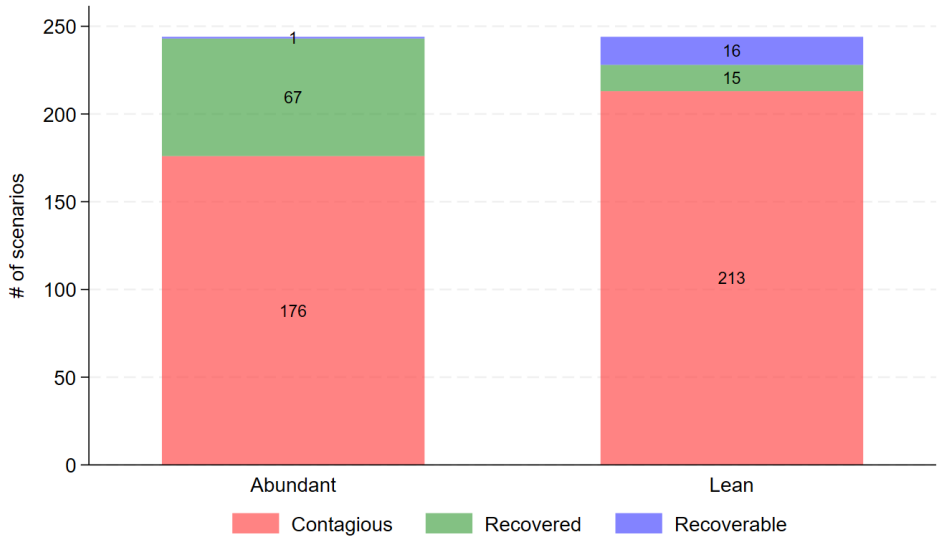

Figure 9: Number of scenarios based on their recovery status, by inventory size.

As expected, the majority of scenarios in both inventory size cases results in contagion from which the supply chain network does not recover by the end of the simulation horizon. However, the figures are clearly different between the two cases. In the lean-inventory one, 213 scenarios, or 87% of them, result in non-recoverable contagion compared to 176, or 72%, in the abundant-inventory case. The difference between the two is more pronounced in the number of recovered scenarios. Notably, non-contagious scenarios are more than twice as many in the abundant-inventory case (68 compared to 31) while this figure increases to 4.5 times if one considers the recovered scenarios (67 to 15) alone.

Naturally, abundant inventories permit companies who experience input shortages from their suppliers to operate without disrupting their own output for a longer period of time. This impedes the contagion's downstream cascade giving time to the flooded companies to recover from the original shock hence reversing the process.

4.3 The role of scenario-specific factors

In addition to the size of firms' inventories which play a fundamental role in the transmission of input disruptions, the study examines the relationship between scenario-specific factors and impact metrics.

[27]Recoverable scenarios are those in which contagion doesn't spread beyond a few companies during the simulation horizon, indicating that full recovery would be likely if given more time.

4.3.1 Initial conditions

One such set of factors are each scenario's initial conditions which determine the severity of the shock by setting the flood magnitude as well as specifying the directly affected companies. These initial conditions include the total number of flooded firms (N_0), the total number of their customers, i.e. their out-degree, (D_0^{out}), their average criticality for their customers' production (C_0^{out}) and the average flood depth among those affected (F_0). The study examines the initial conditions' statistical association with two impact metrics. The first one is the time it requires to reach the high-propagation regime (t_N^*) and characterizes the speed of the contagion's development. The second is the estimated relative output lost (L^*) at the aforementioned point in time.

Table 3 displays the coefficients of the following regression:

$$y_i = b_{1,i}N_{0,i} + b_{2,i}D_{0,i}^{out} + b_{3,i}C_{0,i}^{out} + b_{4,i}F_{0,i} + c_i \quad (1)$$

where the dependent variable is $y = \{t_N^*, L^*\}$ for each inventory size case, i. To examine the difference between the two cases, the analysis runs a pooled regression augmenting each independent variable in the previous equation with an interaction term with an inventory dummy. The latter takes the value of 1 for the abundant inventories and 0 otherwise. Column $\Delta(A-L)$ reports the respective results.

Table 3: Association between scenario impact and its initial conditions.

	t_N^*			L^*		
	Lean	***Abundant***	$\Delta(A-L)$	***Lean***	***Abundant***	$\Delta(A-L)$
N_0	-0.058	-0.046*	0.011	-0.201	0.506**	0.707***
	(0.386)	(0.063)	(0.873)	(0.168)	(0.019)	(0.006)
D_0^{out}	-0.327***	-0.089***	0.239***	0.202*	0.166	-0.036
	(0.000)	(0.000)	(0.000)	(0.081)	(0.340)	(0.862)
C_0^{out}	0.105**	-0.029	-0.134**	0.790***	0.635***	-0.155
	(0.034)	(0.294)	(0.033)	(0.000)	(0.001)	(0.504)
F_0	-0.069***	-0.023**	0.046*	0.219***	0.344***	0.125
	(0.003)	(0.050)	(0.078)	(0.002)	(0.000)	(0.256)
constant	4.288***	6.526***	2.238***	-0.553**	-1.812***	-1.259***
	(0.000)	(0.000)	(0.000)	(0.024)	(0.000)	(0.006)
Num. obs.	199	167		199	167	
R^2	0.636	0.449		0.163	0.297	

Note: N_0 denotes the number of initially affected firms, D_0^{out} their out-degree (i.e. the sum of direct customers), C_0^{out} their average criticality and F_0 the average flood depth. All variables are expressed in natural logarithms. The column $\Delta(A-L)$ denotes the difference in the coefficients between abundant and lean inventories. Heteroskedastic robust standard errors are used and p-values reported in parentheses. ***/**/* indicates significance at the 1/5/10 percent level.

The results in Table 3 are largely in line with intuition. The out-degree of the initially affected firms and flood depth are always negatively associated with the onset of the high-propagation regime, t_N^*. Interestingly, the coefficients in the abundant inventory case are statistically smaller compared to the lean inventory one. This indicates that while these variables correlate with a faster development of the contagion, the strength of that link depends on the size of firms' inventories. A similar pattern appears in the relative output lost, L^*. Flood depth is a statistically significant correlate along with average criticality and, less importantly, with out-degree. However, contrary to the t_N^*, the coefficients' magnitude does not statistically differ between the two inventory size cases. Finally, the number of initially affected firms does seem to play a role only in the abundant inventory case in both impact metrics. The existence of a statistically significant relationship between N_0 and impact variables in

only one of the two inventory cases could suggest the presence of a threshold effect with respect to the former. It may indicate that lean inventories require a higher number of initially affected firms in order exhibit a detectable link with the relevant impact variables, while this is already visible in the abundant-inventory one.

4.3.2 Geographical origin of shocks

In addition to the initial conditions, another scenario-specific factor is crucial: the affected supply chain branches. This is determined by the scenario applied and, in particular, the companies involved in the impacted supply chain as well as the order by which they are affected.

A way to study this is by examining each scenario's impact severity, by the disruption's geographical origin. As location is the primary determinant of which supply chains will be affected, this is a coarse way to analyse the branch-specific impact and identify the most vulnerable supply chains.

Table 4 presents the descriptive statistics of t_N^* and L^*, grouped by continent and broken down by inventory size.

Table 4: Descriptive statistics of t_N^* and L^*, by scenarios' continent of origin and inventory size.

Continent	Inventory	**Min**		**Mean**		**Median**		**Max**		**N**
		t_N^*	L^*	t_N^*	L^*	t_N^*	L^*	t_N^*	L^*	
Asia	*Abundant*	282	0	485.5	1.6	453	1	801	4.1	61
	Lean	5	0	27.7	1.4	20	0.8	98	7.4	69
Europe	*Abundant*	267	0	541.3	1.1	501.5	0.4	1234	3.9	62
	Lean	3	0	35.2	1.1	23	0.5	189	5	74
North America	*Abundant*	319	0	539.8	1.2	521	0.7	1232	4	48
	Lean	6	0	44.6	1.3	32	0.6	163	6.9	65
Oceania	*Abundant*	390	0	614.3	1.2	702	0.4	751	3.1	3
	Lean	15	0.1	23.7	1.9	24	0.4	32	5.3	3
South America	*Abundant*	567	0	612	0.1	612	0.1	657	0.1	2
	Lean	24	0.1	30	0.6	30	0.6	36	1.1	2

Note: t_N^* in days and L^* in % of original output.

The output in Table 4 indicates that scenarios originating in Asian countries are, by and large, more impactful; they exhibit lower t_N^*s, i.e. contagion develops faster, and the higher L^*s suggest heavier relative output losses. The previous pattern holds for both metrics and inventory sizes. From the remaining scenarios, Europe-originating ones generally exhibit a quicker pace in the contagion's spread but the associated losses are on par or smaller compared to those from North America. Finally, the other two continents have too few scenarios to draw representative continent-related conclusions. Nevertheless, the scenarios from Oceania show non-trivial impact, comparable to the European ones. Appendix F presents a more detailed picture of individual scenarios' ranking for the two impact metrics discussed, by continent of flood's origin.

4.4 Sectoral impact

The previous analysis suggests that shocks have a heterogeneous impact on the network's aggregate output depending on the supply chain affected. In addition to impact heterogeneity depending on the scenarios' origin, the study examines the sectoral impact expressed as relative output loss by a sector's companies as a share of the respective sector's original output (L_s^*), at $t = t_N^*$. Since the impact is stronger for the lean-inventory case, the subsequent analysis focuses on it.

Figure 10 shows the distribution of L_s^* across scenarios, by NACE 2-digit sector, clustered into four groups with respect to the highest L_s^* ($L_{max,s}^*$) reached across scenarios.

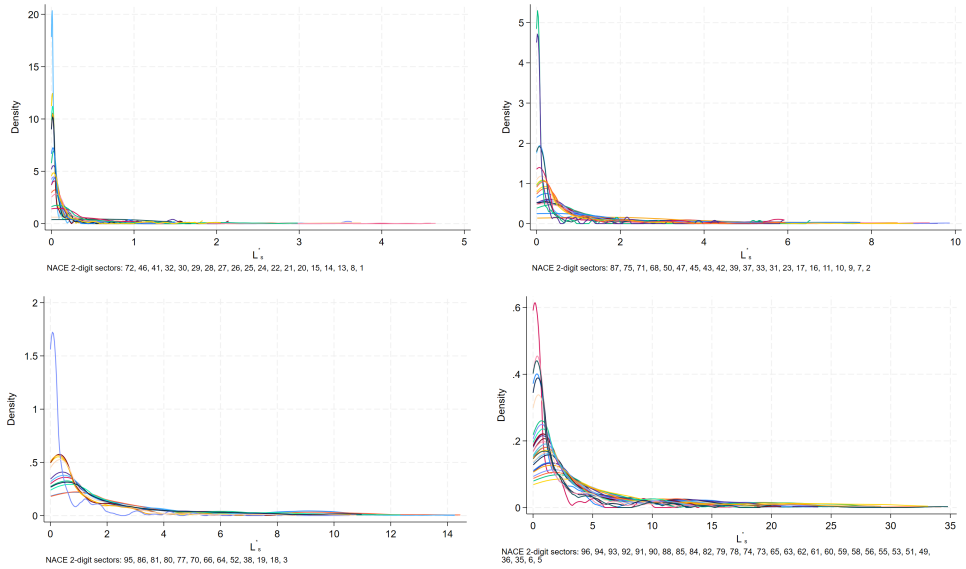

Figure 10: Kernel density plots of sectoral L^*'s distribution across flood scenarios, by NACE 2-digit sector. Distributions are clustered into four groups depending on the $L_{max,s}^*$ reached. Top row (left) up to 5% and (5%, 10%] (right). Bottom row (left) (10%, 15%] and beyond 15% (right).

The long, right tails of the distributions in Figure 10 indicate that the majority of flood scenarios have a small impact and only very few result in extreme losses, until t_N^*. This pattern holds across sectors although the level of these losses differs. However, this difference in the maximum relative output lost reveals the existence of sectoral heterogeneity. This is better presented in Figure 11 which breaks down each NACE section (i.e. NACE 1-digit sectors) by the $L_{max,s}^*$ reached from its constituent sub-sectors (i.e. NACE 2-digit ones).

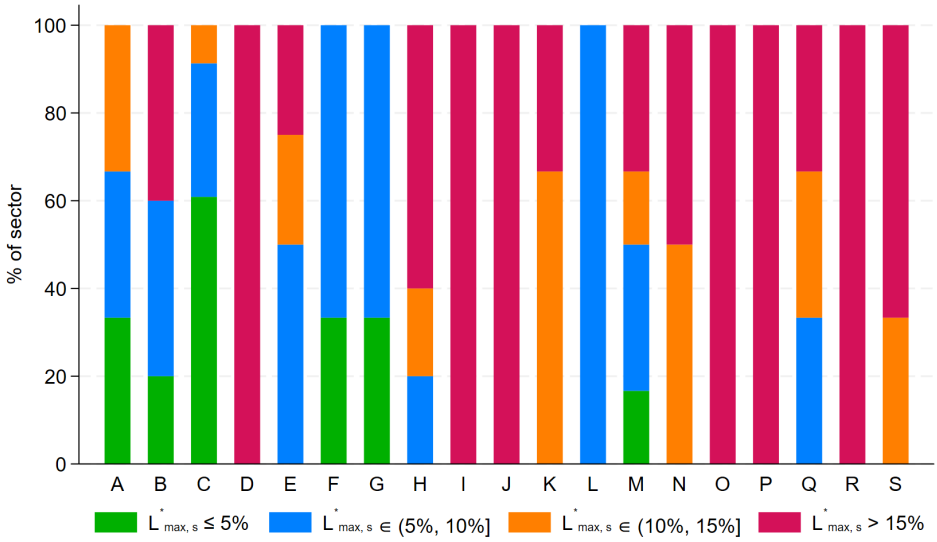

Figure 11: Share of NACE 1-digit sectors by $L^*_{max,s}$ reached across scenarios from its constituent 2-digit sub-sectors.

Figure 10 shows that the NACE 1-digit sectors which experience the highest impact are mostly associated with service activities. With the exception of two sectors, most sub-sectors from sectors H to S exhibit $L^*_{max,s}$s higher than 10% in at least one flood scenario. On the contrary, sectors on the industrial and trade sides of the activity spectrum are more moderately impacted, showing maximum sectoral L^*s of at most 10% and often even below 5%. For example, in the manufacturing sector (C), 14 and 7 sub-sectors exhibit $L^*_{max,s}$s of at most 5% and 10%, respectively, while only 2 exceed 10%. Similarly, in the construction sector (F), two sub-sectors show maximum sectoral output losses beyond 5% but up to 10% (42: civil engineering, 43: specialised construction activities) while the remaining one has an $L^*_{max,s}$ of below 5% (43: construction of buildings).

There are four relevant sources of heterogeneity which could contribute to the emergence of this pattern. Firm-specific attributes which could manifest at a sub-sector level. These include companies' inventory size, the number of their suppliers (i.e. their in-degree) and the latter's criticality. As seen above, larger inventories curb the shock's transmission. Also, higher input criticality could intuitively result in higher losses, in case critical suppliers experience large losses themselves. In-degree's effect could be two-sided. On the one hand, the impact could be diluted in case of a high number of suppliers. However, having many suppliers means that there are many sources for a shock's transmission. At an aggregate level, the size of each 2-digit sector could mitigate the average impact as the latter would spread among more individuals. Figure 12 shows a visual representation of the association between $L^*_{max,s}$ and the various factors, by NACE 2-digit sector.

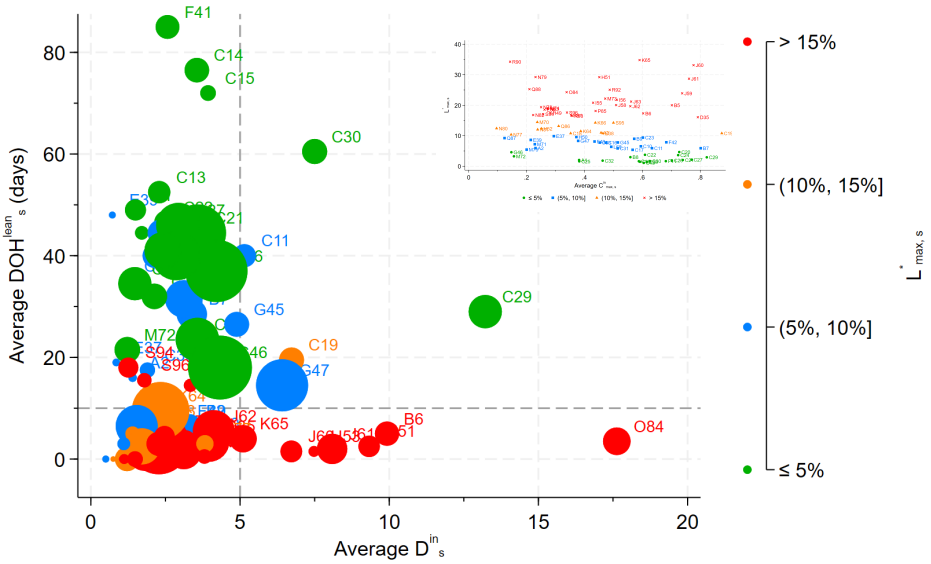

Figure 12: Main plot: Association between $L^*_{max,s}$ and average inventory size (DOH^{lean}_s), in-degree (D^{in}_s) and sector size (indicated by marker size). Inlet: Association between $L^*_{max,s}$ and average in-criticality ($C^{in}_{max,s}$), by NACE 2-digit sector. The warmer the color, the higher the impact group.

Figure 12 reveals several interesting patterns. First, it seems that the average inventory size of a sub-sector's firms[28] plays a crucial role. Sub-sectors with average DOH^{lean}_ss beyond 15 days very rarely exhibit high $L^*_{max,s}$s. On the contrary, below that inventory size threshold, most sub-sectors belong to the high-impact group. A mitigating factor seems to be sub-sector size. Highly populated sub-sectors don't exceed 15% in relative output losses even if they exhibit small average inventory sizes. Finally, the results suggest that the higher the average number of suppliers a sub-sector's companies have, the higher the impact they will experience. In particular, the bottom-right area of the plot, with average DOH^{lean}_ss below 15 days and average in-degrees beyond 5, is populated only by high-$L^*_{max,s}$ sub-sectors. Interestingly, average input criticality doesn't seem to be associated with $L^*_{max,s}$. As the inlet in Figure 12 shows, sub-sectors of every impact group spread across the full range of average input criticality, without a specific pattern.

Table 5 shows the respective bi-variate and multivariate relationships between $L^*_{max,s}$ and the various factors examined.

[28] As described above, information on firms' $DOH^{lean}_{i,s}$ is largely imputed as a draw from a uniform distribution between sector s's minimum $DOH_{i,s}$ and its first quartile. Therefore, the figure for sector s's average DOH_s should be $(DOH^{min}_s + DOH^{Q1}_s)/2$, or very close to it depending on the non-imputed information.

Table 5: Association between $L^*_{max,s}$ and sources of sectoral heterogeneity.

	$\mathbf{Corr}(L^*_{max,s}, X)$	$L^*_{max,s} = f(X)$
$\overline{DOH^{lean}_s}$	-0.666***	-0.294***
	(0.000)	(0.000)
$\overline{D^{in}_s}$	0.248**	0.687***
	(0.022)	(0.009)
N_s	-0.230**	-0.166***
	(0.033)	(0.000)
$\overline{C^{in}_{max,s}}$	-0.160	4.336
	(0.142)	(0.244)
constant		14.537***
		(0.000)
Num. obs.	86	86
R^2		0.547

Note: $\overline{DOH^{lean}_s}$ denotes the average (lean) inventory size of a sub-sector s's firms, $\overline{D^{in}_s}$ their average in-degree (i.e. the average number of suppliers), $\overline{C^{in}_{max,s}}$ their average in-criticality and N_s is the sub-sector's size (expressed in 100 companies). Heteroskedastic robust standard errors are used in the regression and p-values reported in parentheses. ***/**/* indicates significance at the 1/5/10 percent level.

The results in Table 5 are the quantitative equivalent of Figure 12. Both pairwise correlation and linear regression coefficients, reported in the first and second column respectively, confirm that average sectoral inventory time and in-degree are statistically significantly associated with $L^*_{max,s}$, along with sub-sector size. On the contrary, average sectoral in-criticality doesn't show a statistically significant link with sectoral output loss.

4.5 An early warning indicator

Among the various factors which influence the propagation of shocks along the supply chain, firms' criticality exhibits an interesting property. In particular, the average of affected firms' maximum out-criticality ($\overline{C^{out}_{max}}$) consistently peaks ahead of the high-contagion regime's onset thus acting as an early warning indicator. Figure 13 plots the distribution of the difference (Δ^*) between the time to high-contagion regime's start (t^*_N) and $\overline{C^{out}_{max}}$'s peak (t^*_C) across scenarios, by inventory size.

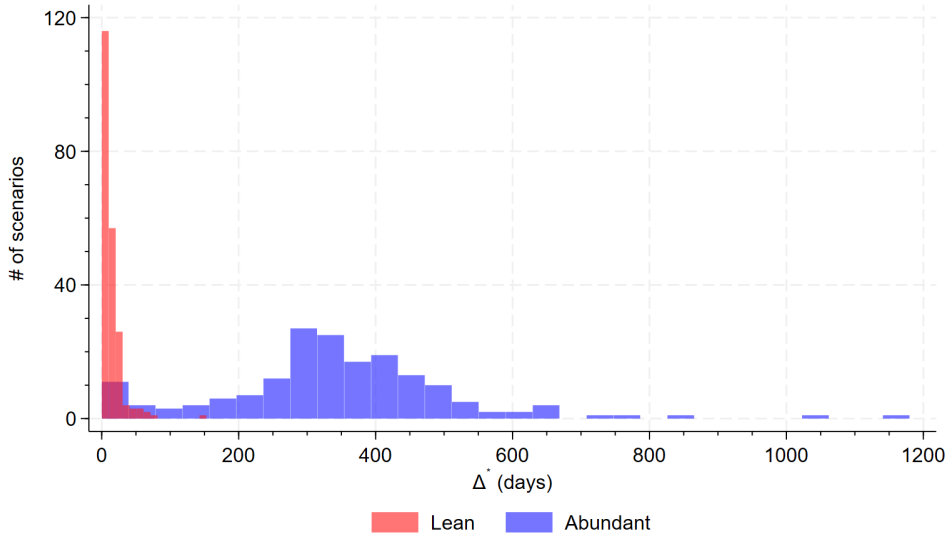

Figure 13: Distribution of scenarios based on their $\Delta^* = t_N^* - t_C^*$, by inventory size.

As seen in Figure 13, Δ^* is always positive, with each distribution showing a distinct spread, by inventory size. More precisely, t_C^* precedes t_N^* by 13 days, on average, for the lean inventory case while this figure rises to almost a year in the abundant inventory one. Arguably, two weeks is a short time-frame to implement actions which would effectively prevent the disruption's downstream cascade. However, the two to five hundred days by which t_C^* predates t_N^* in most scenarios in an abundant inventory world, should provide ample reaction time for both companies and policy-makers to design and implement mitigating measures. Therefore, monitoring this indicator in real-time and identifying the moment it peaks could give an early warning about a forthcoming rapid spread of production shortages. How early, would depend on the size of companies' actual inventories. Finally, ranking scenarios by their Δ^* provides information about which would require swift action, if feasible, in case shocks materialize and which ones would allow for a more careful planning and less urgency. The last part of Appendix F presents a detailed picture and a short description of the results.

5 Discussion

The study investigated the indirect impact of extreme flood events through the cascade of production disruptions across the global supply chain. It combined various types of company-level data from multiple sources with flood hazard maps and integrated them into a network, agent based model to probe the mechanism of shocks' propagation and identify some of the factors that influence it.

The simulations suggest that the size of inventories is a fundamental factor for the transmission of production disruptions through the supply chain. In a lean-inventory world shocks spread substantially faster and result in higher losses and fewer recoveries than in an abundant-inventory one.

While the effect of firms' inventory size transcends every aspect of the analysis, the simulations revealed several factors that shape shocks' downstream cascade. These include company-level attributes which are intertwined with scenario-specific parameters and their influence manifests at macro level.

The number and criticality of flooded companies' outgoing trade links correlate positively with a faster pace and more severe impact of contagion, respectively. Moreover, flood magnitude is positively associated with both faster shock transmission and

more severe impact.

Geographically, flood events originating in Asian countries develop faster and result in higher output losses. Floods in Europe exhibit the second fastest contagion but their impact on global supply chain's losses is comparable to or smaller than those in North America. The differences among continents are more pronounced in the abundant-inventory case for both impact metrics: contagion speed and relative output loss.

From a sectoral perspective, companies engaging in industrial and trade-related activities, i.e. NACE sectors A, B, C, E, F and G, are generally less heavily impacted compared to those in services. The analysis shows that the magnitude of maximum sectoral output loss decreases as the number of a sector's constituent companies and their inventory sizes increase, while it increases with a higher number of suppliers.

Finally, the study identified an indicator which shows an interesting property: the average of affected firms' maximum out-criticality peaks consistently before the shock's propagation enters its fast-pace regime. The duration of the related early-warning period, as every other factor, strongly depends on the size of companies' inventories.

Overall, the analysis exposed a, well-known yet fundamental weakness of the lean-inventory management system which is its potential to facilitate the transmission of shocks through the supply chain (Ortiz, 2022). This highlights the importance of keeping large enough inventories, especially for companies which are deemed to be of critical nature for a country's or continent's productive capacity.

Importantly, the developed model enables the assessment of input shortages' impact and the identification of the most vulnerable supply chains to production disruptions. While this study primarily examines shocks stemming from extreme flood events, the model can simulate the cascade of shocks of broader origin, such as trade restrictions driven by geopolitical factors.

It should be noted that the results provide a ballpark direction and magnitude of extreme flood events' effect due to a number of data availability and modelling challenges.

From a data perspective, a common (Inoue and Todo, 2019), yet key limitation is the lack of locational information at factory-level which would provide a more accurate identification of the originally flooded companies. Nevertheless, it is very challenging to collect precise information on that, worldwide. Indeed, the very few studies which employ such information focus on very specific supply chains, within a single or very small number of countries (Tabachová et al., 2024; Schueller et al., 2022; Burgos and Ivanov, 2021). Another piece of information which is very scarce or, at best, very fragmented at a global level is the trade volume -in monetary or other terms- between trade partners. However, the study addresses this issue in two ways; using a production function which has been found to provide an adequate approximation of shocks' propagation, when compared to that of a firm network with link weights based on trade volume information Chakraborty et al. (2024) and; using a survey-based, expert judgment assessment of input criticality as a proxy of trade relationships' importance Pichler et al. (2022). Although useful, there are two associated caveats with the latter: input criticality has been assessed: a) for a developed economy's companies, thus it might be less representative for those from a developing one and b) at a rather coarse industry level, hence it might not appropriately capture links' importance at more granular level. Finally, the global focus of the current study limits the sample mostly to large, listed companies as trade relationship information for SMEs is virtually inaccessible at international level.

The model also involves some simplifying assumptions which in general, imply that the results of the analysis are on the conservative side.

The first assumption is that a firm cannot substitute the missing inputs from its affected suppliers, neither by forming new trade links nor by receiving extra input from relevant, non-affected ones. This suggests that the network's structure and firms' productive capacity remains constant during the simulation.

The model starts with a data-driven representation of the global supply chain network at a specific point in time which remains stable throughout the simulation. The absence of the formation of new trade links among affected companies (i.e. re-wiring of the network) should capture the actual behaviour of firms in a satisfactory manner, at least in the short-run. Indeed, empirical research has shown that trade partnerships remain stable in the event of natural disasters hitting one of the parties involved, especially in the case of highly specialized products and/or temporary shocks (Martin et al., 2023; Freund et al., 2022; Arriola et al., 2020; Boehm et al., 2019). This suggests that the simulated impact is on the more severe side, i.e. if idle supply and idle demand were matched, this would result in lower contagion and, thus, impact. An associated assumption to the static network's structure, is that firms' productive capacity remains constant. Hence, non-affected, supplying firms cannot increase their output to cover their customers' additional demand. This also implies that the results correspond to a worst-case scenario, in which firms produce specific, non-substitutable products.

An additional static aspect in the simulation is the size of companies' inventories. Firms in the model do not actively manage their inventories, e.g. by expanding it in case of anticipated shortages. Nevertheless, by examining the two polar cases of lean and abundant inventories, the study provides a range within which the dynamic inventory management results should lie.

Finally, the current implementation of the model considers only downstream shock propagation. Although reverse transmission of the shock is possible, research has found that downstream effects are more important when production functions are non-linear (Diem et al., 2022).

An extension of the current study would be to re-examine the results when plant-level location information becomes available. Intuitively, this would result in floods exhibiting a more widespread effect, but possibly of smaller magnitude as the impact of each event would spread among many factories.

A more general extension would be to consider the combined impact of more types of natural disasters such droughts or wildfires. Although such an exercise would be very data-demanding and computationally challenging, the result would provide a more accurate picture of the impact of climate-related natural disasters.

6 Conclusion

Alarmingly, the most recent evidence indicate that global warming will likely result to a 2.6 °C to 3.1 °C temperature rise by the end of the century which will increase the frequency and intensity of climate-related natural disasters (UNEP, 2024).

This study has shown that the ripple effect of such disasters can spread much farther than its place of origin and have its impact amplified by its transmission through the global supply chain network. At the same time, the analysis identified several factors which can mitigate the adverse effects and even issue an early warning, before the shock's transmission enters a high-pace regime.

Importantly, the study provided a framework which, when combined with more granular and higher quality data, could improve the resilience of the supply chain network against a range of risks, beyond natural disasters.

References

Acemoglu, D., Ozdaglar, A., and Tahbaz-Salehi, A. (2015). Systemic risk and stability in financial networks. *American Economic Review*, 105(2):564–608.

Amaral, A., Connell Garcia, W., Di Cometi, F., and Herghelegiu, C. (2022). 'SCAN' (Supply Chain Alert Notification) monitoring system. *Single Market Economics Papers*.

Arriola, C., Guilloux-Nefussi, S., Koh, S.-H., Kowalski, P., Rusticelli, E., and Van Tongeren, F. (2020). Efficiency and risks in global value chains in the context of COVID-19.

Auer, R. A., Levchenko, A. A., and Sauré, P. (2019). International inflation spillovers through input linkages. *Review of Economics and Statistics*, 101(3):507–521.

Barrot, J.-N. and Sauvagnat, J. (2016). Input specificity and the propagation of idiosyncratic shocks in production networks. *The Quarterly Journal of Economics*, 131(3):1543–1592.

Battiston, S., Caldarelli, G., May, R. M., Roukny, T., and Stiglitz, J. E. (2016). The price of complexity in financial networks. *Proceedings of the National Academy of Sciences*, 113(36):10031–10036.

Boehm, C. E., Flaaen, A., and Pandalai-Nayar, N. (2019). Input linkages and the transmission of shocks: Firm-level evidence from the 2011 Tōhoku earthquake. *Review of Economics and Statistics*, 101(1):60–75.

Bonnet, P. and Ciani, A. (2023). Applying the SCAN methodology to the semiconductor supply chain. *JRC Working Papers in Economics and Finance*.

Burgos, D. and Ivanov, D. (2021). Food retail supply chain resilience and the COVID-19 pandemic: A digital twin-based impact analysis and improvement directions. *Transportation Research Part E: Logistics and Transportation Review*, 152:102412.

Carvalho, V. M., Nirei, M., Saito, Y. U., and Tahbaz-Salehi, A. (2021). Supply chain disruptions: Evidence from the Great East Japan earthquake. *The Quarterly Journal of Economics*, 136(2):1255–1321.

Chakraborty, A., Reisch, T., Diem, C., Astudillo-Estévez, P., and Thurner, S. (2024). Inequality in economic shock exposures across the global firm-level supply network. *Nature Communications*, 15(1):3348.

Diem, C., Borsos, A., Reisch, T., Kertész, J., and Thurner, S. (2022). Quantifying firm-level economic systemic risk from nation-wide supply networks. *Scientific reports*, 12(1):7719.

Diem, C., Borsos, A., Reisch, T., Kertész, J., and Thurner, S. (2024). Estimating the loss of economic predictability from aggregating firm-level production networks. *PNAS nexus*, 3(3):pgae064.

Dolgui, A. and Ivanov, D. (2021). Ripple effect and supply chain disruption management: new trends and research directions. *International Journal of Production Research*, 59(1):102–109.

Dolgui, A., Ivanov, D., and Sokolov, B. (2018). Ripple effect in the supply chain: an analysis and recent literature. *International journal of production research*, 56(1-2):414–430.

Dottori, F., Alfieri, L., Salamon, P., Bianchi, A., Feyen, L., and Hirpa, F. (2016). Flood hazard map of the world - 100-year return period [dataset]. Technical report, European Commission, Joint Research Centre (JRC). PID: http://data.europa.eu/89h/jrc-floods-floodmapgl$_rp100y - tif$.

Fahr, S., Senner, R., and Vismara, A. (2024). The globalization of climate change: Amplification of climate-related physical risks through input-output linkages.

FEMA (2011). Hazus 2.1 flood model technical manual. *Federal Emergency Management Agency, Department of Homeland Security, Washington, DC, USA*.

FEMA (2022). Hazus 5.1 flood model technical manual. *Federal Emergency Management Agency, Department of Homeland Security, Washington, DC, USA*.

Forslid, R. and Sanctuary, M. (2023). Climate risks and global value chains: The impact of the 2011 Thailand flood on Swedish firms.

Freund, C., Mattoo, A., Mulabdic, A., and Ruta, M. (2022). Natural disasters and the reshaping of global value chains. *IMF Economic Review*, 70(3):590.

Glasserman, P. and Young, H. P. (2015). How likely is contagion in financial networks? *Journal of Banking & Finance*, 50:383–399.

Glasserman, P. and Young, H. P. (2016). Contagion in financial networks. *Journal of Economic Literature*, 54(3):779–831.

Hallegatte, S. (2019). Disasters' impacts on supply chains. *Nature sustainability*, 2(9):791–792.

Haraguchi, M. and Lall, U. (2013). Flood risks and impacts future research questions and implication to private investment decision-making for supply chain networks. *Background paper prepared for the global assessment report on disaster risk reduction.*

Haraguchi, M. and Lall, U. (2015). Flood risks and impacts: A case study of Thailand's floods in 2011 and research questions for supply chain decision making. *International Journal of Disaster Risk Reduction*, 14:256–272.

Huang, X., Vodenska, I., Havlin, S., and Stanley, H. E. (2013). Cascading failures in bi-partite graphs: model for systemic risk propagation. *Scientific reports*, 3(1):1219.

Huizinga, J., De Moel, H., and Szewczyk, W. (2017). Global flood depth-damage functions. methodology and the database with guidelines. *EUR 28552 EN, Publications Office of the European Union, Luxembourg.*

Inoue, H. and Todo, Y. (2019). Firm-level propagation of shocks through supply-chain networks. *Nature Sustainability*, 2(9):841–847.

Ivanov, D. and Dolgui, A. (2022). Stress testing supply chains and creating viable ecosystems. *Operations Management Research*, 15(1):475–486.

Jackson, M. O. and Pernoud, A. (2021). Systemic risk in financial networks: A survey. *Annual Review of Economics*, 13(1):171–202.

Lehner, B. and Grill, G. (2013). Global river hydrography and network routing: Baseline data and new approaches to study the world's large river systems. *Hydrological Processes*, 27(15):2171–2186.

Martin, J., Mejean, I., and Parenti, M. (2023). Relationship stickiness, international trade, and economic uncertainty. *Review of Economics and Statistics*, pages 1–45.

Ortiz, J. L. (2022). Spread too thin: The impact of lean inventories. *International Finance Discussion Paper*, (1342).

Ozdagli, A. K. and Weber, M. (2023). Monetary policy through production networks: Evidence from the stock market. *Fama-Miller Working Paper, Chicago Booth Research Paper*, (17-31).

Pichler, A., Pangallo, M., del Rio-Chanona, R. M., Lafond, F., and Farmer, J. D. (2022). Forecasting the propagation of pandemic shocks with a dynamic input-output model. *Journal of Economic Dynamics and Control*, 144:104527.

Ramani, V., Ghosh, D., and Sodhi, M. S. (2022). Understanding systemic disruption from the COVID-19-induced semiconductor shortage for the auto industry. *Omega*, 113:102720.

Schueller, W., Diem, C., Hinterplattner, M., Stangl, J., Conrady, B., Gerschberger, M., and Thurner, S. (2022). Propagation of disruptions in supply networks of essential goods: A population-centered perspective of systemic risk. *arXiv preprint arXiv:2201.13325*.

Simchi-Levi, D. and Simchi-Levi, E. (2020). We need a stress test for critical supply chains. *Harvard Business Review*, 28.

Summer, M. (2013). Financial contagion and network analysis. *Annu. Rev. Financ. Econ.*, 5(1):277–297.

Tabachová, Z., Diem, C., Borsos, A., Burger, C., and Thurner, S. (2024). Estimating the impact of supply chain network contagion on financial stability. *Journal of Financial Stability*, 75:101336.

Tellman, B., Sullivan, J. A., Kuhn, C., Kettner, A. J., Doyle, C. S., Brakenridge, G. R., Erickson, T. A., and Slayback, D. A. (2021). Satellite imaging reveals increased proportion of population exposed to floods. *Nature*, 596(7870):80–86.

UNEP (2024). *Emissions Gap Report 2024: No more hot air ... please!*

Vodenska, I., Dehmamy, N., Becker, A. P., Buldyrev, S. V., and Havlin, S. (2021). Systemic stress test model for shared portfolio networks. *Scientific reports*, 11(1):3358.

List of Figures

List of Tables

Appendix

A River flood hazard maps

The study uses the river flood hazard maps at global scale developed by Dottori et al. (2016). They represent flood-prone areas globally for potential river flood events of six different magnitudes. A common expression of a flood's magnitude is through its return period.[29] This metric reflects how often a flood of a certain magnitude is matched or exceeded in a specified time interval. Figure 14 shows an example of flood hazard maps of 1-in-10-, 1-in-100- and 1-in-500-year return periods. Each cell in the has a resolution of approximately 1 square kilometer and the associated values indicate water depth in meters.

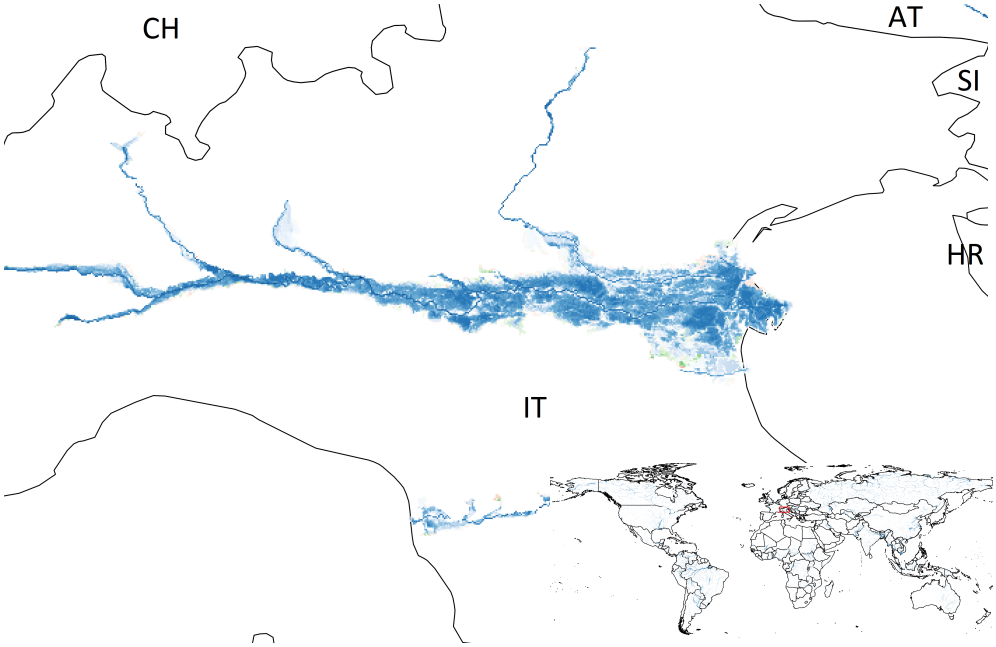

Figure 14: Detail of global map flood hazard maps of 1-in-10-year (blue shades), 1-in-100-year (green shades) and 1-in-500-year (red shades) return periods around river Po. Inlet: Global flood hazard maps of the same return periods. Country boundaries layer by the World Bank Official Boundaries dataset.

As seen in Figure 14 the three events show a considerable overlap and they spatially extend from each other by a small margin. Table 6 shows the descriptive statistics of the floods' magnitude for the available return periods.

Table 6: Descriptive statistics of flood events' water depth for different return periods.

Return period	**Min**	**Max**	**Mean**	**Std. Dev.**
1-in-10 year	0.01	30.00	3.18	4.80
1-in-20 year	0.01	30.00	3.28	4.85
1-in-50 year	0.01	30.00	3.40	4.93
1-in-100 year	0.01	30.00	3.48	4.98
1-in-200 year	0.01	30.00	3.56	5.03
1-in-500 year	0.01	30.00	3.67	5.09

Note: Based on flood hazard map data by the Joint Research Centre and authors' calculations.

[29] Also known as *recurrence frequency* or *recurrence interval*.

As can be seen from Table 6, the average flood depth reached from the least extreme events to the most extreme ones differs by roughly 50 cm while the return periods span from 1-in-10 to 1-in-500 years. The increase over the range of the various event frequencies is very gradual, by increments of about 10 cm each. This indicates a very modest variation along the magnitude dimension. Table 7 shows the descriptive statistics of countries' flooded area percentage for events of various return periods.

Table 7: Descriptive statistics of flood events' country coverage for different return periods.

Return period	**Min**	**Max**	**Mean**	**Std. Dev.**
1-in-10 year	0.00	38.89	3.54	4.73
1-in-20 year	0.00	41.33	3.75	5.01
1-in-50 year	0.00	43.48	3.97	5.29
1-in-100 year	0.00	44.91	4.12	5.47
1-in-200 year	0.00	46.15	4.25	5.63
1-in-500 year	0.00	47.63	4.41	5.83

Note: Based on flood hazard map data by the Joint Research Centre, country boundaries by the World Bank Official Boundaries dataset and authors' calculations.

Table 7 indicates that, on average, floods would cover around 4% of countries' surface. However, the increase over the different return periods is non-trivial; average figures rise by almost 1 percentage point while the maxima by about 10 times as much. Moreover, the range reveals that large heterogeneity exists across countries. The top 5 countries in terms of flooded area shares are Bangladesh, the Netherlands, South Sudan, Hungary and Gambia.

B River basin information

The boundaries and areas of river basins globally come from the HydroBASINS database (Lehner and Grill, 2013). It contains global information of river sub-basins which are consistently sized and hierarchically nested in 12 breakdown levels.

Each one contains a number of different sub-basins of various areas. Table 8 presents the average and median sub-basin area (in km^2) per breakdown level as well as their numbers.

Table 8: Global river sub-basin area statistics.

Breakdown level	**Mean area (km^2)**	**Median area (km^2)**	**N**
1	14719395.50	15914618.00	9
2	2176340.25	1782085.50	61
3	461198.71	263478.51	288
4	101781.79	57233.30	1305
5	28632.30	17534.90	4639
6	8252.58	5338.90	16095
7	2382.37	1574.90	55764
8	720.95	487.60	184285
9	268.54	204.00	494750
10	143.74	138.60	924328
11	130.92	135.40	1014817
12	130.63	135.40	1017093

Note: Based on HydroBASINS data and authors' calculations.

Data in Table 8 show that at the least granular scale, the database includes 9 individual sub-basins with an the average area of almost 15 million km^2 while in the

opposite side of the breakdown spectrum there are more than 1 million sub-basins with an average area of 130.63 km^2. To choose an appropriate sub-basin breakdown scale for grouping the flood hazard map data, the study uses information from Tellman et al. (2021) who provide estimates of flood extent for 913 large flood events from 2000 to 2018 based on satellite imagery. The average estimated flooded area covers about 6890 km^2 while the median is close to 2100 km^2. Comparing these figures with those in Table B, breakdown levels 6 and 7 yield the closest matches to the average and median areas, respectively.

Combined with flood hazard and company information, the first one results in 244 distinct river basins which, on average, encompass 7 firms with around 6.5 customers (out-links) each. The average water depth reached in the affected firms' locations is almost 4 meters. By comparison, the respective figures for the 7th breakdown level are 5 firms with about 8.5 customers and the same water depth. Given the similarities between the two, this study uses the former to generate individual scenarios of spatially grouped, flooded companies.

C Depth-damage curves

To assess the direct damage caused by a flood event to the impacted companies, the study uses the global depth-damage curves developed by Huizinga et al. (2017). Their advantage is that they provide consistent, continent-specific, depth-damage curves which allow supra-national flood damage assessments.

Each damage-curve indicates the fractional damage of water depth for different damage classes broadly including residential buildings (e.g. houses and apartments), commercial buildings (e.g. offices, schools, hospitals, hotels, shops), industrial buildings (e.g. warehouses, distribution centers, factories), transport facilities, infrastructure (roads and railroads) and agricultural lands.

To operationalize these damage-curves, this study classifies each company into one of the three most relevant damage classes; agriculture; commercial; and industrial buildings. Table 9 provides an overview of the mapping between each damage class and the corresponding NACE classification.

Table 9: Allocation of NACE sectors into structure damage classes.

Damage class	**NACE sector(s)**	**Short description**	**Sample percentage**
Agriculture	A	Agriculture, forestry & fishing	0.68
Industrial buildings	B - F	Mining, manufacturing, electricity, gas & water supply, construction	48.71
Commercial buildings	G - U	Trade, transportation, accommodation, ICT, financial & real estate, professional & administrative, health services, public sector	50.61

Note: Sectoral classification information is missing for about 6% of the sample. These companies have been allocated in the industrial damage class.

The analysis estimates the functional form of each damage-curve as a simple sigmoid function of the following form:

$$D_{i,j} = \frac{1}{1 + e^{(-a_{i,j} \cdot f + b_{i,j})}}$$

, where f the water depth and $D_{i,j}$ the damage factor indicating the fractional damage caused to damage class $i = \{agriculture, commercial, industrial\}$ located in conti-

nent $j = \{Africa, Asia, NorthAmerica, South/CentralAmerica, Europe, Oceania\}$. Figures 15 to 17 show the estimated damage functions and the underlying data for each continent and relevant damage class.

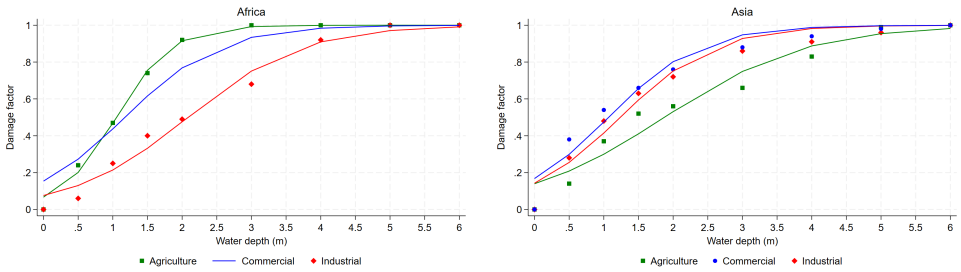

Absent continent-specific data for commercial building structures in Africa, the analysis relies on the respective global damage-curve to estimate the relevant damage function.

Figure 15: Damage functions for Africa (left) and Asia (right) for agriculture, commercial and industrial building structures.

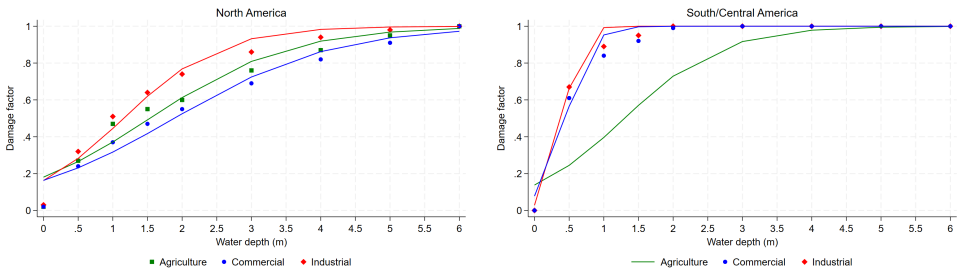

Absent continent-specific data for agricultural lands in South/Central America, the analysis relies on the respective global damage-curve to estimate the relevant damage function.

Figure 16: Damage functions for North (left) and South/Central America (right) for agriculture, commercial and industrial building structures.

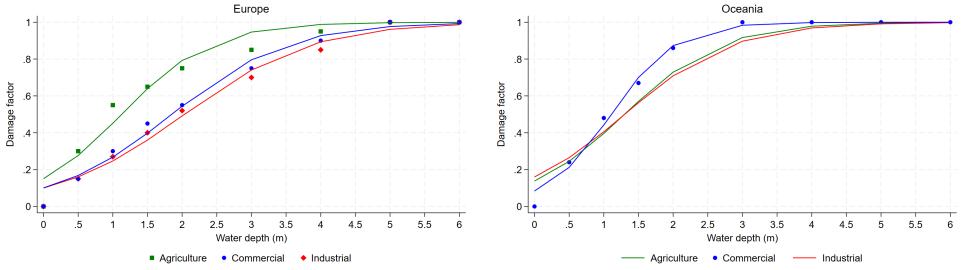

Absent continent-specific data for agricultural lands and industrial buildings in Oceania, the analysis relies on the respective global damage-curves to estimate the relevant damage functions.

Figure 17: Damage functions for Europe (left) and Oceania (right) for agriculture, commercial and industrial building structures.

This study quantifies the damage caused to each flooded company in a consistent manner using the estimated coefficients of the respective damage functions.

D Recovery time

Information on recovery times is very scarce and substantially fragmented in the literature, probably reflecting the challenge to obtain reliable estimates for a sufficiently wide range of cases. The Federal Emergency Management Agency (FEMA) provides such information for a broad variety of building structures allowing its consistent application.

In particular, the Hazus flood model (FEMA, 2022) has estimates of the maximum restoration time (in days) as a step-function of water depth for different building types. They are developed based on expert judgement and take into account a number of processes such as time for physical repair of the damage, inspection time, permit and their approval time and contractor availability. Building type classification is more detailed compared to the damage functions', including several types in each broad class of residential, commercial and industrial buildings. In total, there are 33 available building structure types.

A mapping of the relevant, mostly non-residential building types, to Standard Industrial Classification (SIC) codes facilitates the association of each company into a specific building type and its respective restoration time. The sample of potentially flooded firms in this study and their associated building types correspond to ten categories of restoration time functions. Table 10 shows the allocation of SIC codes into the different restoration time categories based on Hazus model's scheme (FEMA, 2011).

Table 10: Allocation of SIC codes into restoration time classes.

TTR class	**SIC codes**	**Short description**	**Sample percentage**
1	72, 75, 76, 83, 88	Personal & repair services	0.63
2	70	Temporary lodging	0.68
3	40, 41, 43-47, 49, 60-65, 67, 73, 78 (except 7832), 80 (except 8062, 8063, 8069), 81, 82, 87, 89, 91-97	Business, professional, financial and health services, government, education	30.98
4	42, 48, 50-59, 7832, 79, 84, 86	Retail & wholesale trade, entertainment services	12.83
5	8062, 8063, 8069	Hospitals	0.77
6	1, 2, 7-9, 22, 24, 26, 32, 34, 35 (except 3571, 3572), 37	Agriculture, heavy industry	16.08
7	15-17, 23, 25, 27, 30, 31, 36 (except 3671, 3672, 3674), 38, 39	Light industry, construction	14.77
8	20, 21, 28, 29	Food, drugs, chemicals industry	16.12
9	10, 12-14, 33	Metals, minerals processing industry	4.92
10	3571, 3572, 3671, 3672, 3674	High technology	2.21

Note: SIC information is missing for about 2% of the potentially flooded company sample. These companies have been allocated in the 8th TTR class.

In addition to the information in Table 10, Figure 18 presents the associated maximum recovery time functions for each group of building structures.

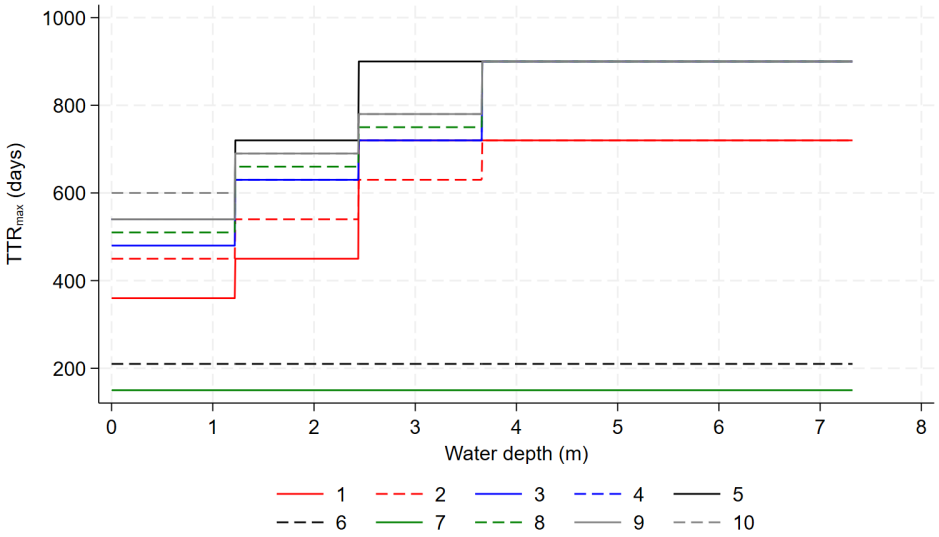

Figure 18: Maximum time-to-recover per building structure group (TTR class) based on Hazus model (FEMA, 2011, 2022) data.

Figure 18 indicates that, generally, maximum restoration times increase with water depth with the exception of building structure groups 6 and 7 which show a flat TTR_{max} pattern. Another observation is that the water depth beyond which every recovery time peaks, and remains stable afterwards, is 4 meters. This number is lower for the hospital class for which TTR_{max} reaches its maximum is about 2.5 meters. Finally, Figure 18 highlights the rationale for allocating companies with missing SIC code information in the 8th restoration time group. The latter exhibits a balanced pattern among the available ones.

E Example of production disruption propagation

Figure 19 provides a detailed example of a production shock's downstream cascade, based on the mechanism and the production function described in the main text.

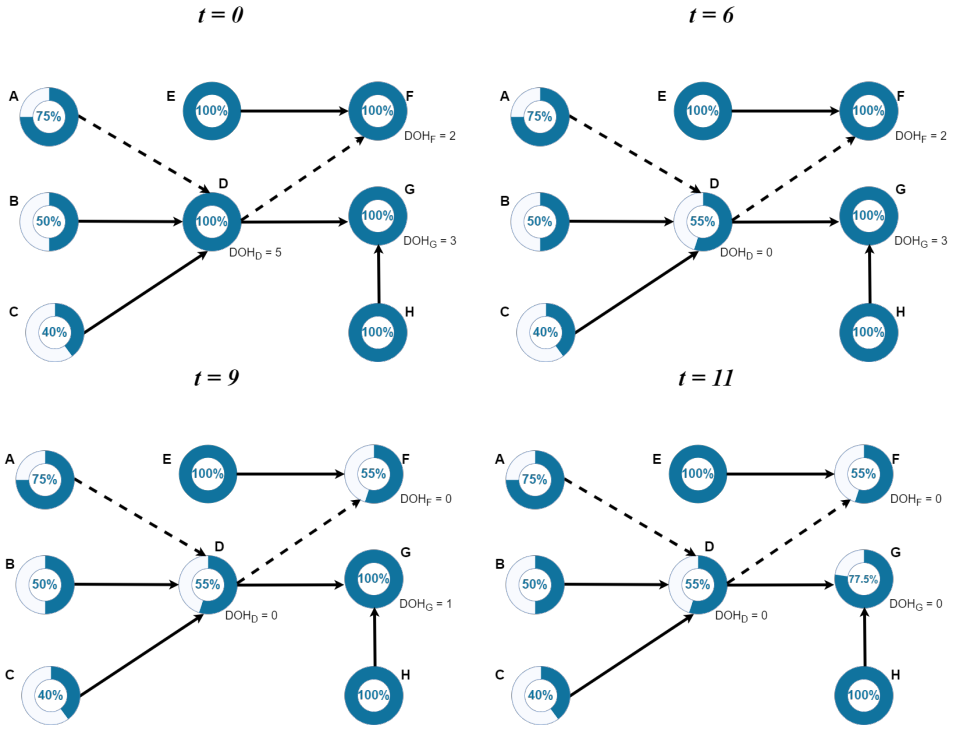

Figure 19: Example of shock propagation originating in companies A, B and C through a supply chain network of eight nodes. Dashed links represent critical trade relationships while solid links, non-critical ones. Numbers in the nodes denote their relative production, compared to the undisrupted network.

A flood of certain magnitude affects at $t = 0$ companies A, B and C causing a reduction of their production levels to 75%, 50% and 40% of the original, respectively, based on an assumed damage-function. Company A is a critical supplier for company D's production while B and C supply company D with non-critical inputs. After five time steps during which company D maintains its original production level utilizing its inventories ($DOH_D = 5$), it is forced to reduce its output to 55% (i.e. $x_D(6) = min\left(0.75, \frac{0.75+0.5+0.4}{3}\right)$). Subsequently, company F exhausts its inventory in the following two time steps ($DOH_F = 2$) and reduces its relative production to 55%, too (i.e. $x_F(9) = min\left(0.55, \frac{0.55+1}{2}\right)$). Company G which has only non-critical inputs and one additional day of available inventory ($DOH_G = 3$) gets affected last, experiencing a loss of 22.5% compared to its original production level.

To illustrate the cascade of the shock, this example assumes that flooded companies' TTRs are greater than the days of inventory of their customers. Obviously, if a company recovers, the propagation mechanism results in the reverse outcome.

F Ranking of scenarios according to t_N^*, L^* and Δ^*, by inventory size

Figures 20 and 21 show the full distribution of scenarios' impact metrics, colored by the continent of the flood's origin and broken down by inventory size.

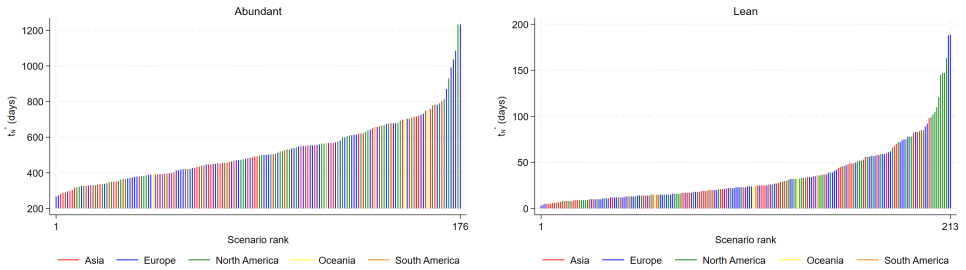

Figure 20: Ranking of scenarios according to the time needed to reach the high-contagion regime for abundant (left panel) and lean (right panel) inventory sizes. Each line corresponds to an individual scenario. Red spikes indicate scenarios originating in Asia, blue in Europe, green in North America, yellow in Oceania and orange in South America. Order is from the most to the least severe scenario.

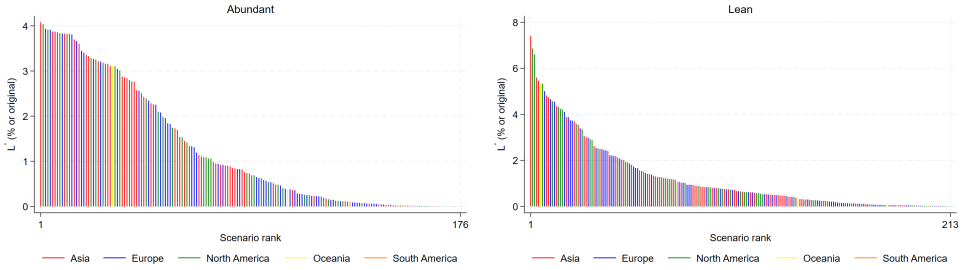

Figure 21: Ranking of scenarios according to the relative output lost at t_N^* for abundant (left panel) and lean (right panel) inventory sizes. Each line corresponds to an individual scenario. Red spikes indicate scenarios originating in Asia, blue in Europe, green in North America, yellow in Oceania and orange in South America. Order is from the most to the least severe scenario.

The graphs in Figures 20 and 21 reveal the existence of large heterogeneity as well as a substantial decline in severity across scenarios, especially in the lean-inventory case. The patterns from the full distributions are in line with the aggregate statistics presented in Table 4. In general, scenarios originating in Asia and North America exhibit the highest losses while several from the European ones are among those with the fastest spread of the disruption, i.e. the lowest t_N^*.

Finally, Figure 22 plots the ranking of scenarios, according to the duration of their early warning period, Δ^*.

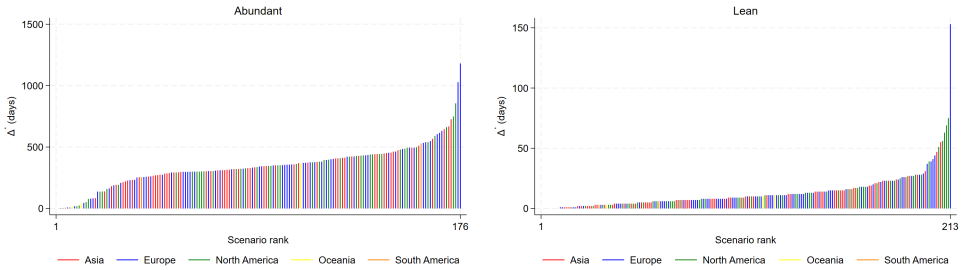

Figure 22: Ranking of scenarios according to Δ^* for abundant (left panel) and lean (right panel) inventory sizes. Each line corresponds to an individual scenario. Red spikes indicate scenarios originating in Asia, blue in Europe, green in North America, yellow in Oceania and orange in South America. Order is from the most to the least severe scenario.

As seen in Figure 22, scenarios originating in Asian countries generally rank high in severity, e.g. exhibit short Δ^*s. However, the topmost positions in both lean and abundant inventories are occupied by Europe- and North America-originating scenarios. This is particularly prominent in the lean-inventory case where the top ten scenarios are not visible in the plot because their $\Delta^* = 0$. Out of those, seven originate in North America and the rest in Asia.

A noteworthy, general pattern is the distinct shape of the distributions between the two inventory size cases. In every metric, distributions exhibit a sharper change in the lean-inventory case compared to a more gradual adjustment in the abundant one. Moreover, their magnitude points out the higher severity of the lean-inventory case. Transmission times and early warning periods are an order of magnitude shorter while impact is twice as high.

Getting in touch with the EU

In person

All over the European Union there are hundreds of Europe Direct centres. You can find the address of the centre nearest you online (european-union.europa.eu/contact-eu/meet-us_en).

On the phone or in writing

Europe Direct is a service that answers your questions about the European Union. You can contact this service:

— by freephone: 00 800 6 7 8 9 10 11 (certain operators may charge for these calls),

— at the following standard number: +32 22999696,

— via the following form: european-union.europa.eu/contact-eu/write-us_en.

Finding information about the EU

Online

Information about the European Union in all the official languages of the EU is available on the Europa website (european-union.europa.eu).

EU publications

You can view or order EU publications at op.europa.eu/en/publications. Multiple copies of free publications can be obtained by contacting Europe Direct or your local documentation centre (european-union.europa.eu/contact-eu/meet-us_en).

EU law and related documents

For access to legal information from the EU, including all EU law since 1951 in all the official language versions, go to EUR-Lex (eur-lex.europa.eu).

EU open data

The portal data.europa.eu provides access to open datasets from the EU institutions, bodies and agencies. These can be downloaded and reused for free, for both commercial and non-commercial purposes. The portal also provides access to a wealth of datasets from European countries.

Science for policy

The Joint Research Centre (JRC) provides independent, evidence-based knowledge and science, supporting EU policies to positively impact society

EU Science Hub
Joint-research-centre.ec.europa.eu